Journal of Medical Microbiology (2012), **61**, 820–829 DOI 10.1099/jmm.0.041137-0

Molecular epidemiology of the attachment glycoprotein (G) gene in respiratory syncytial virus in children with acute respiratory infection in Japan in 2009/2010

Ayako Yoshida,[1] Naoko Kiyota,[2] Miho Kobayashi,[3] Koichi Nishimura,[2] Rika Tsutsui,[1] Hiroyuki Tsukagoshi,[3] Eiko Hirano,[4] Norio Yamamoto,[5] Akihide Ryo,[6] Mika Saitoh,[3] Seiya Harada,[2] Osamu Inoue,[1] Kunihisa Kozawa,[3] Ryota Tanaka,[7] Masahiro Noda,[8] Nobuhiko Okabe,[8] Masato Tashiro,[5] Katsumi Mizuta[9] and Hirokazu Kimura[3,8]

Correspondence
Hirokazu Kimura
kimhiro@nih.go.jp *or*
hkimura0511@gmail.com

[1]Aomori Prefectural Institute of Public Health and Environment, 1-1-1 Higashitsukurimichi, Aomori-shi, Aomori 030-8566, Japan

[2]Kumamoto Prefectural Institute of Public Health and Environmental Sciences, 1240-1 Kurisaki-machi, Uto-shi, Kumamoto 869-0425, Japan

[3]Gunma Prefectural Institute of Public Health and Environmental Sciences, 378 Kamioki-machi, Maebashi-shi, Gunma 371-0052, Japan

[4]Fukui Prefectural Institute of Public Health and Environmental Science, 39-4 Harame-cho, Fukui-shi, Fukui 910-8551, Japan

[5]Influenza Virus Research Center and Infectious Disease Surveillance Center, National Institute of Infectious Diseases, 4-7-1 Gakuen, Musashimurayama-shi, Tokyo 208-0011, Japan

[6]Department of Molecular Biodefence Research, Yokohama City University Graduate School of Medicine, 3-9 Fukuura, Kanazawa-ku, Yokohama-shi, Kanagawa 236-0004, Japan

[7]Department of Surgery, Institute of Medical Sciences, Kyorin University, 6-20-2 Shinkawa, Mitaka-shi, Tokyo 181-8611, Japan

[8]Infectious Disease Surveillance Center, National Institute of Infectious Diseases, 4-7-1 Gakuen, Musashimurayama-shi, Tokyo 208-0011, Japan

[9]Yamagata Prefectural Institute of Public Health, 1-6-6 Toka-machi, Yamagata-shi, Yamagata 990-0031, Japan

Received 30 November 2011
Accepted 25 February 2012

This study performed a detailed genetic analysis of the glycoprotein (*G*) gene of respiratory syncytial virus (RSV) detected in 50 Japanese children with acute respiratory infection (ARI) in the 2009/2010 season. A phylogenetic tree constructed by the neighbour-joining method showed that 34 and 16 of the RSV strains could be classified into subgroups A and B, respectively. Strains belonging to subgroups A and B were further subdivided into GA2 and BA, respectively. The nucleotide and deduced amino acid sequence identities were relatively high among these strains (>90 %). The deduced amino acid sequences implied that a relatively high frequency of amino acid substitutions occurred in the C-terminal 3rd hypervariable region of the G protein in these strains. In addition, some positively selected sites were estimated. The results suggest that RSV with genotypes GA2 and BA was associated with ARI in Japanese children in 2009/2010.

Abbreviations: AdV, Adenovirus; ARI, acute respiratory infection; CI, confidence interval; EV, enterovirus; FEL, fixed effects likelihood; HBoV, human bocavirus; HMPV, human metapneumovirus; HPIV, human parainfluenza virus; HRV, human rhinovirus; IFEL, internal fixed effects likelihood; NJ, neighbour-joining; REL, random effects likelihood; RSV, respiratory syncytial virus; SLAC, single likelihood ancestor counting.

The GenBank/EMBL/DDBJ accession numbers for the nucleotide sequences determined in this study are AB683188–AB683237.

INTRODUCTION

Respiratory syncytial virus (RSV) in the genus *Pneumovirus* and family *Paramyxoviridae* causes acute respiratory infection (ARI) in children (Peter & James, 2006; Vardas *et al.*, 1999). RSV infection may cause major problems in infants <1 year of age and can lead to life-threatening ARIs such as bronchiolitis and bronchopneumonia (Leung *et al.*, 2005; Shay *et al.*, 1999; Yorita *et al.*, 2007). In addition, recent studies have shown that RSV infections may be associated with the initiation or exacerbation of asthma (Pérez-Yarza *et al.*, 2007; Sigurs *et al.*, 2000).

The RSV genome encodes ten proteins (Peter & James, 2006). Among these, the attachment glycoprotein (G) is a major structural protein and may be associated with both infectivity and antigenicity (Anderson *et al.*, 1985; Johnson *et al.*, 1987; Rueda *et al.*, 1991). Previous reports suggest that the amino acid sequences of the G protein show both conservative and hypervariable regions (Cane *et al.*, 1991). The highly conserved region is mainly a receptor-binding region between aa 164 and 176, whilst the C-terminal 3rd hypervariable region is situated around positions 210–290 (Botosso *et al.*, 2009). This region contains multiple epitopes for neutralizing antibodies (Palomo *et al.*, 1991). Indeed, there may be a mass of sites under positive selection in this region. In addition, the G protein partially mimics a chemokine (CX3C) as well as fractalkine (a chemokine, CX3CL1) (Tripp *et al.*, 2001). Thus, it is important to analyse the G protein to obtain a better understanding of the properties of RSV.

Molecular epidemiological studies have shown that RSV can be classified into two phylogenetic subgroups, RSV-A and RSV-B (Mufson *et al.*, 1985). The strains of subgroup A can be subclassified into eight genotypes (GA1–GA7 and SAA1), as can those of subgroup B (BA, GB1–GB4 and SAB1–3) (Parveen *et al.*, 2006). A recent study showed that subgroup A genotypes GA1, GA2, GA5 and GA7, and subgroup B genotype BA have been detected in the USA (Rebuffo-Scheer *et al.*, 2011). In addition, our recent studies suggest that GA2, GA5 and BA are detected in most Japanese infants with ARI (Fujitsuka *et al.*, 2011; Goto-Sugai *et al.*, 2010; Nakamura *et al.*, 2009). However, the molecular epidemiology of RSV remains to be clarified. Phylogenetic methods such as neighbour-joining (NJ) are frequently used to analyse the molecular epidemiology of various virus genomes. The NJ method is based on an algorithm that enables cluster analysis and evaluation of the rate of virus evolution (Kimura, 1980; Saitou & Nei, 1987). In addition, the maximum-likelihood method provides an estimation of the time rate of virus evolution (Felsenstein, 1981; Gojobori *et al.*, 1990). Using these methods, we conducted a detailed genetic analysis of the *G* gene in RSV isolates detected from children with ARI in Japan in the 2009/2010 season.

METHODS

Samples and patients. Nasopharyngeal swabs (n=709) were collected from patients with ARI. The patients were diagnosed with common cold, influenza-like illness, bronchitis, bronchiolitis, wheezy bronchiolitis and pneumonia. Samples were obtained by the local health authorities of the Aomori (northern Japan, n=14), Gunma (central Japan, n=332) and Kumamoto (southern Japan, n=363) prefectures for the surveillance of viral diseases in Japan between September 2009 and April 2010. A distance of 500–1200 km separates each sampled area. Informed consent was obtained from parents or guardians to perform sampling. We primarily isolated various viruses from the samples using cell-culture methods for Vero E6, RD18S and Madin–Derby canine kidney cells. Next, in the samples negative for isolation, we detected various respiratory viruses such as influenza A (H1N1) pdm09 virus, seasonal influenza virus (subtypes A, B and C), human parainfluenza virus (HPIV; types 1–4), adenovirus (AdV), human rhinovirus (HRV), human metapneumovirus (HMPV), enterovirus (EV) and human bocavirus (HBoV) by (RT)-PCR, as described previously (Allander *et al.*, 2005; Bellau-Pujol *et al.*, 2005; Echevarría *et al.*, 1998; Miura-Ochiai *et al.*, 2007; Nakauchi *et al.*, 2011; Olive *et al.*, 1990; Takao *et al.*, 2004; Zhang & Evans, 1991). In addition, we attempted to isolate and/or detect various respiratory bacteria such as *Haemophilus influenzae*, *Legionella pneumophila*, *Neisseria* spp. and *Bordetella pertussis* by culture and *Streptococcus* spp. using a kit (Bisno *et al.*, 1997). We also detected *Mycoplasma pneumoniae* by PCR (Nadala *et al.*, 2001). None of these bacteria was isolated or detected in any of the samples.

RNA extraction and RT-PCR for detection of RSV. Samples were centrifuged at 3000 *g* at 4 °C for 30 min, and viral RNA were extracted from the 140 µl supernatant using a QIAamp Viral RNA Mini kit (Qiagen). Reverse transcription was performed using a PrimeScript RT Reagent kit (Takara Bio) according to the manufacturer's instructions. RT-PCR of the RSV *G* gene was carried out with the following primers: forward primer ABG490 (5′-ATGATTWYCA-YTTTGAAGTGTTC-3′, corresponding to nt 497–519 of the *G* gene of reference strain A2 and nt 491–513 of reference strain 18537) and reverse primer F164 (5′-GTTATGACACTGGTATACCAACC-3′, corresponding to nt 151–173 of the *G* gene of strain A2, and nt 164–186 of the fusion protein gene of strain 18537, with one mismatch with the *G* gene of strain A2; Sullender *et al.*, 1993). PCR was initiated at 94 °C for 1 min, followed by 35 cycles of 94 °C for 40 s, 50 °C for 45 s and 72 °C for 45 s, with a final extension at 72 °C for 10 min. The amplicon sizes were 607/610 bp and 670 bp for group A/B and BA viruses, respectively. The PCR product was purified with a QIAquick PCR Purification kit (Qiagen). The purified products were sequenced using a BigDye Terminator v3.1 Cycle Sequencing kit (Applied Biosystems) using the two primer sets above. Sequence analysis was performed on an ABI PRISM 3130 Genetic Analyzer (Applied Biosystems). General precautions were taken to prevent carry-over contamination of PCR, as described previously (Lam *et al.*, 2007).

Phylogenetic analysis and calculation of pairwise distances (*p*-distances). We analysed the nucleotide sequences (nt 505–894, 390 bp for A2; nt 502–951, 450 bp for reference strain BA4128B/99B) and the deduced amino acid sequences (130 aa for GA2; 150 aa for BA). Phylogenetic analysis of the nucleotide sequence of the *G* gene was conducted using the CLUSTAL W program available from the DNA Data Bank of Japan (http://www.ddbj.nig.ac.jp/index-j.html) and Tree Explorer version 2.12 (http://en.bio-soft.net/tree/TreeExplorer.html). Evolutionary distances were estimated according to Kimura's two-parameter method, and the phylogenetic tree was constructed using the NJ method (Kimura, 1980; Saitou & Nei, 1987). The reliability of the tree was estimated with 1000 bootstrap replications. In addition, we calculated the *p*-distances for the isolated strains to assess the frequency distribution of RSV-A and RSV-B, as described previously (Mizuta *et al.*, 2010).

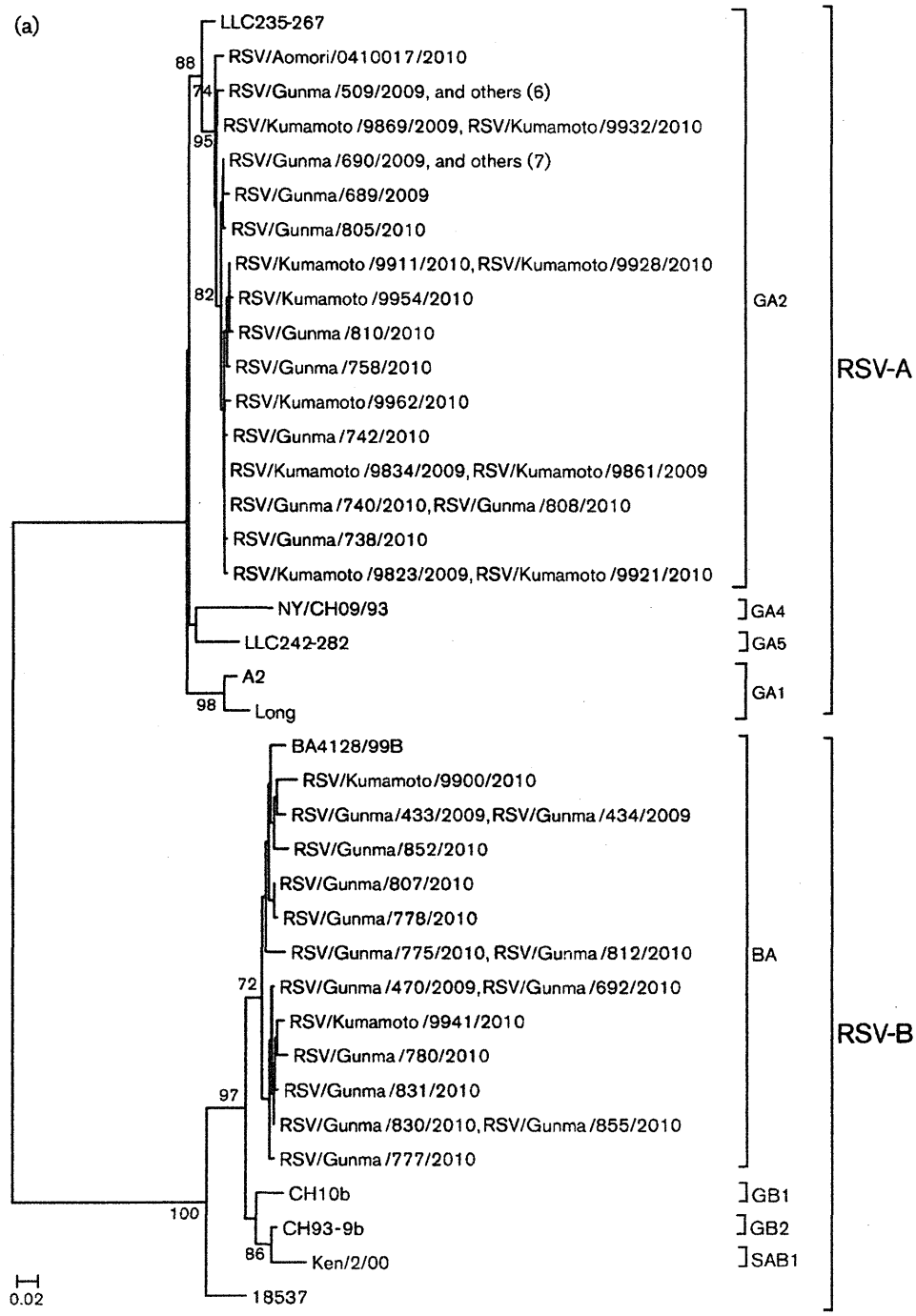

Fig. 1. Phylogenetic trees based on nucleotide sequence (a) and deduced amino acid sequence (b) of the *G* gene. Distance was calculated according to Kimura's two-parameter method and trees were constructed by the NJ method, with labelling of branches showing at least 70% bootstrap support. The GenBank accession numbers of the reference strains are as follows: Long (M17212), A2 (M11486), LLC-235-267 (AY114149), LLC242-282 (AY114150), NY/CH09/93 (AF065254), BA4128/99B (AY333364), CH10b (AF065250), Ken/2/00 (AY524575), CH93-9b (AF065251), and 18537 (M17213). RSV isolates from this study are indicated by the prefix RSV. Bars, 0.02 substitutions per nucleotide position (a); 0.05 amino acid substitutions per site (b).

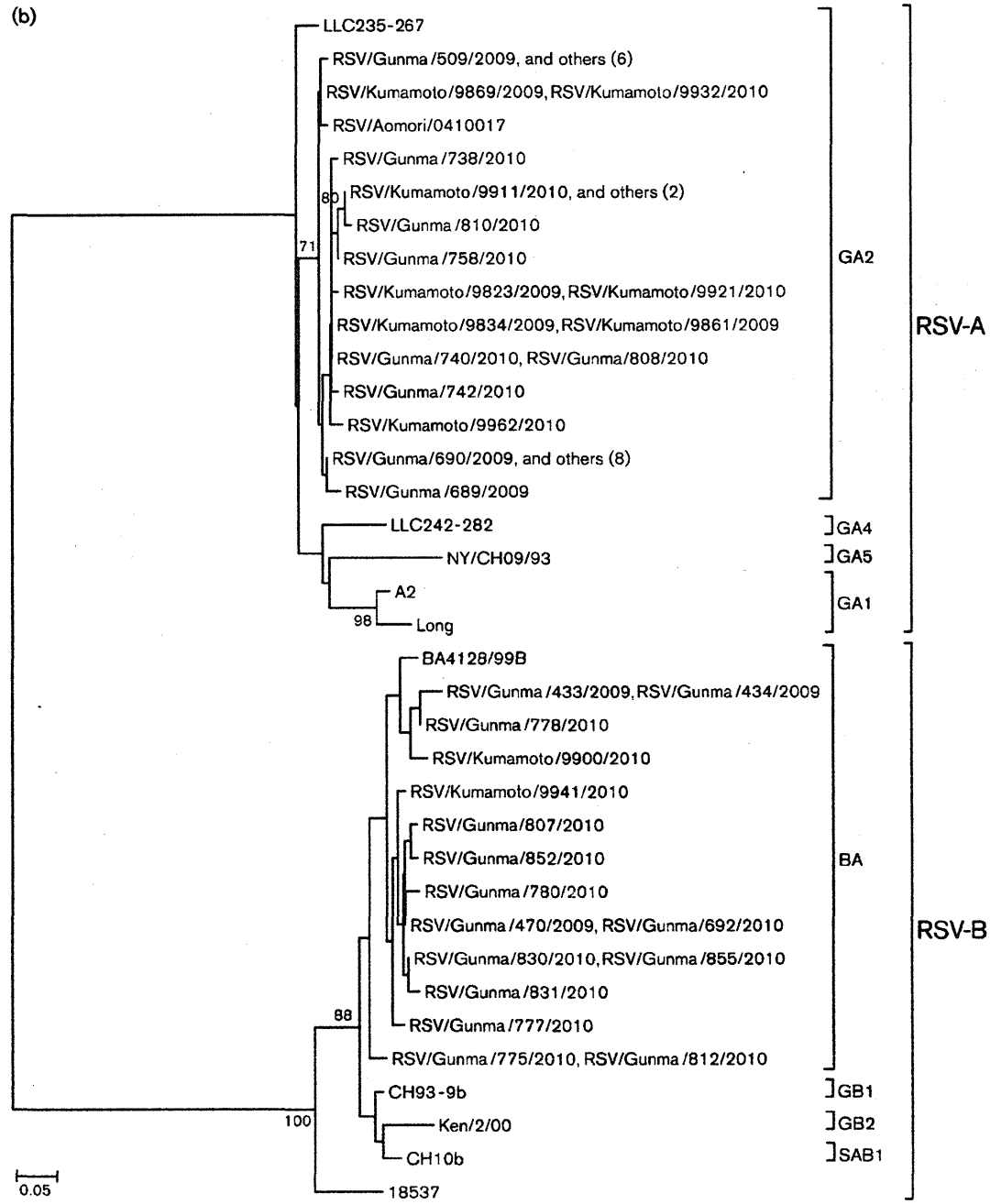

Detection of positively selected sites in the C-terminal 3rd hypervariable region of the G gene and estimation of evolutionary rate. Positive selections were identified using DATAMONKEY (http://www.datamonkey.org) (Pond & Frost, 2005). We used the following four methods to estimate the synonymous (*dS*) and non-synonymous (*dN*) rates at every codon in the alignment: (i) single likelihood ancestor counting (SLAC), (ii) fixed effects likelihood (FEL), (iii) internal fixed effects likelihood (IFEL) and (iv) random effects likelihood (REL). SLAC, FEL and REL methods detect sites under selection at external branches of the phylogenetic tree, whilst the IFEL method investigates sites along the internal branches. Positive selection ($dN>dS$) was determined by a P value of <0.1 (SLAC, FEL and IFEL) or by a Bayes factor of >20 (REL). In addition, we estimated the evolutionary rate for a phylogeny consisting of dated tips. The evolutionary rate is an additional parameter used to scale the times of the internal nodes into units of the expected number of substitutions per site. Phylogenetic analyses by the maximum-likelihood method based on the single rate dated tips model was performed using the TipDate webserver (http://mobyle.pasteur.fr/cgi-bin/portal.py?#forms::tipdate; Rambaut, 2000).

RESULTS

Detection or isolation of RSV and other viruses, and seasonal variations of RSV

We attempted the genetic detection and isolation of RSV, influenza virus, HPIV, AdV, HRV, HMPV, EV, HBoV and

bacteria in samples obtained from 709 Japanese patients with ARI. Although no RSV was isolated in the samples, RSV alone was detected by RT-PCR in 50 patients with ARI (7.1 %) and was prevalent from January to February in 2010. These RSV-positive patients were diagnosed mainly with bronchitis, bronchiolitis and pneumonia. The number of isolates and amplicons detected by performing (RT)-PCR on the other viruses was 438 (61.8 %) for influenza A pdm09 virus (H1N1), six (0.8 %) for influenza A virus (H3N2), 25 (3.5 %) for HRV, eight (1.1 %) for HPIV, seven (1.0 %) for EV, 13 (1.8 %) for AdV and three (0.4 %) for HMPV. No HBoV was detected in any of the samples and no viruses were detected in 159 of the samples. RSV and other viruses were detected in patients aged 1.8 ± 2.0 and 11.6 ± 13.0 years (means $\pm$ SD), respectively. No differences attributable to the male-to-female ratio were observed. To understand better the molecular epidemiology of the *G* gene of RSV, we analysed the gene from patients in which only RSV was detected.

Phylogenetic analysis, identity and *p*-distances in the present strains

Phylogenetic trees (NJ method) based on the nucleotide and deduced amino acid sequences of the *G* gene are shown in Fig. 1(a, b). The tree enabled classification of 34 and 16 strains into subgroups RSV-A and RSV-B, respectively. In addition, the strains in this study could be subdivided into two genotypes (GA2 and BA, Fig. 1). The predominant strains belonged to RSV-A. RSV-A and RSV-B strains shared 97.7–100 and 94.2–100 % nucleotide sequence identity, and 94.4–100 and 91.7–100 % amino acid sequence identity, respectively. In addition, we calculated the *p*-distance between the strains in this study (Fig. 2). The *p*-distance values of RSV-A and RSV-B at the nucleotide level were 0.010 ± 0.006 and 0.028 ± 0.017 (mean $\pm$ SD), respectively, whilst those at the amino acid level were 0.023 ± 0.012 and 0.041 ± 0.024, respectively. The *p*-distance values between RSV-A and RSV-B were not significant. These results suggested that the prevalent RSV strains in the 2009/2010 season in Japan were highly homologous.

Substitutions in the C-terminal hypervariable region, positively selected sites and rate of molecular evolution of the *G* gene in the RSV isolates

The amino acid sequences of RSV-A and RSV-B were compared with the prototype Long and BA4128/99B strains, respectively (Fig. 3a, b). We confirmed amino acid substitutions in the deduced sequences in the G protein and estimated the positively selected sites in the C-terminal 3rd hypervariable region of the protein using the SLAC, FEL, IFEL and REL methods. We estimated that four sites in the RSV-A strains isolated in this study (Asn250Ser, Met262Glu, Arg297Lys and Arg297Glu) were under positive selection by the REL method. The IFEL method estimated that Asn273Tyr and Leu274Pro of HRV-A, and Leu237Pro of RSV-B were under positive selection. We estimated the rate of molecular evolution of the *G* gene in RSV-A as 1.92×10^{-3} substitutions per site per year [95 % confidence interval (CIs) of 2.62×10^{-4}–3.55×10^{-3}] and as 3.59×10^{-3} substitutions per site per year in RSV-B (95 % CI 1.55×10^{-3}–5.59×10^{-3}). The results suggested that the C-terminal hypervariable region of the G protein in the present RSV-A and RSV-B strains had some positively selected sites with high rates of molecular evolution.

DISCUSSION

We conducted a molecular epidemiological study of the *G* gene in RSV detected from Japanese patients with various ARIs such as upper respiratory infection, bronchiolitis, bronchitis, influenza-like illness and pneumonia in the 2009/2010 season. RSV was detected in 7 % (50 of 709 nasopharyngeal swabs) of patients with ARI in the present study. Among these strains, phylogenetic analysis showed that 34 and 16 strains could be classified into genotype GA2 of RSV-A and genotype BA of RSV-B, respectively. The identities of nucleotide and amino acid sequences of these RSV-A and RSV-B isolates were high (>90 %). Some positively selected sites in the C-terminal 3rd hypervariable region of the *G* gene were estimated. In addition, the rate of molecular evolution of the region might be high. Although we analysed a relatively small number of RSV strains, such strains might have been associated with ARIs in the 2009/2010 season in Japan.

The G protein is a major antigen of RSV (Peter & James, 2006). This protein includes a hypervariable region with regard to epitopes for neutralizing antibodies in the C-terminal 3rd hypervariable region of the protein (Palomo *et al.*, 1991). In addition, frequent amino acid substitutions, as positively selected sites, might exist in this region (Woelk & Holmes, 2001). Previous reports suggest that there are 29 sites under positive selection in RSV-A (Botosso *et al.*, 2009). In the present study, we estimated some positively selected sites in the region. Specifically, Asn250Ser, Met262Glu, Arg297Lys and Arg297Glu substitutions in the RSV-A strains were estimated by the REL method, and Asn273Tyr and Leu274Pro substitutions of HRV-A, as well as the Leu237Pro substitution of RSV-B, were estimated by the IFEL method. Furthermore, it is possible that differences in the positively selected sites in the hypervariable region are a result of primary or secondary infection by RSV (Gaunt *et al.*, 2011). In general, primary RSV infection occurs in children <2 years old, whilst most secondary RSV infections are seen in children >2 years old (Glezen *et al.*,1986; Hall, 2004). When primary infection occurred in patients <2 years old in the present study, no differences in the positively selected sites in the detected viruses were found between primary and secondary infection cases (data not shown).

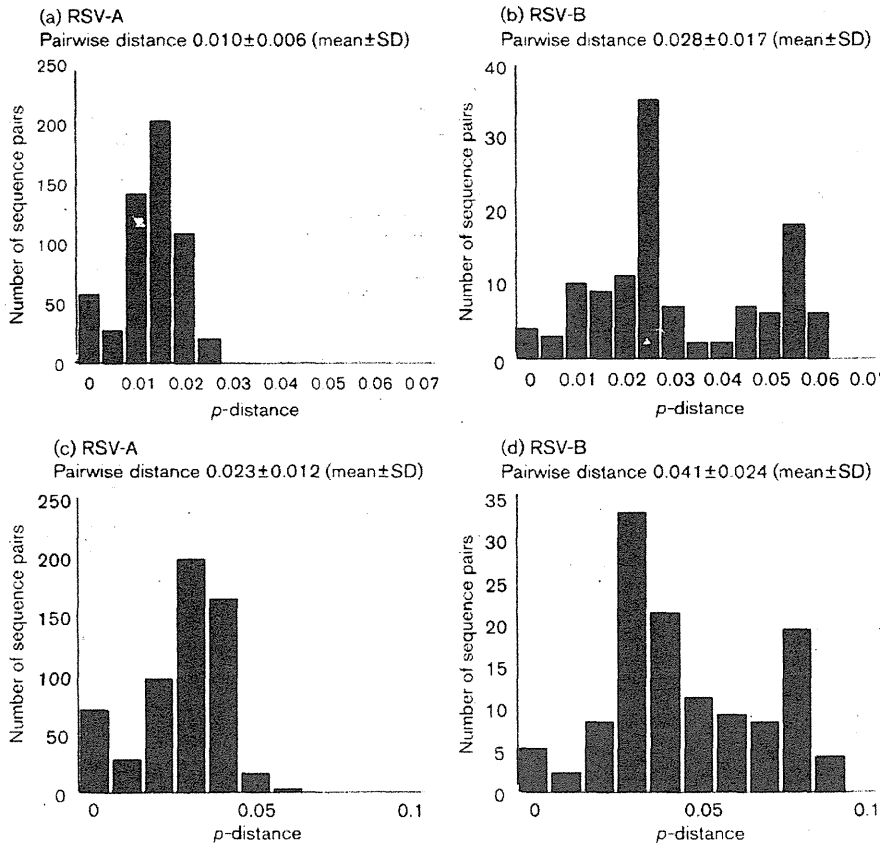

Fig. 2. Distribution of *p*-distances based on the nucleotide sequences of the RSV *G* gene for RSV-A (a) and RSV-B (b) and on the deduced amino acid sequences for RSV-A (c) and RSV-B (d).

In general, the evolutionary rate of structural protein-coding genes may be faster than non-structural protein-coding genes in various viruses (Yeo *et al.*, 2007). Previous reports suggest that every virus shows a unique rate of evolution of structural protein-coding genes. For example, the rate of evolution of the haemagglutinin gene in seasonal influenza virus subtype A (H1N1) is estimated at 1.7×10^{-3} substitutions per site per year (Furuse *et al.*, 2010; Graham *et al.*, 2011). In contrast, the evolutionary rate of the haemagglutinin–neuraminidase-coding region of HPIV-1, another paramyxovirus, is relatively slow (7.68×10^{-4} substitutions per site per year; Mizuta *et al.*, 2011). In the present study, the evolutionary rate of the C-terminal hypervariable region in RSV-A was 1.92×10^{-3} substitutions per site per year and 3.59×10^{-3} substitutions per site per year in RSV-B. These rates are faster than those of previous reports (Zlateva *et al.*, 2004, 2005). This may be because we estimated for the hypervariable region in the C-terminal one-third of the protein, whilst other authors analysed other coding regions, including relatively conservative regions (Zlateva *et al.*, 2004, 2005).

Previous reports suggest that RSV is prevalent during the autumn/winter season in a number of countries including Japan (Reiche & Schweiger, 2009; Sato *et al.*, 2005). For example, Fujitsuka *et al.* (2011) showed that RSV detected during this season may be associated with wheezy bronchiolitis in Japanese infants. Thus, our results appear to be consistent with those of previous studies.

In conclusion, RSV strains detected in samples from patients with ARI in the 2009/2010 season in Japan appeared to be highly homologous and exhibited a high evolutionary rate of the *G* gene. Moreover, these strains had some positively selected sites in the G protein. Thus, these RSV strains may have been associated with various ARIs in Japan during the investigation period.

ACKNOWLEDGEMENTS

This work was partly supported by a Grant-in-Aid from the Japan Society for the Promotion of Science and for Research on Emerging and Re-emerging Infectious Diseases from the Ministry of Health, Labour and Welfare, Japan.

(a) RSV-A

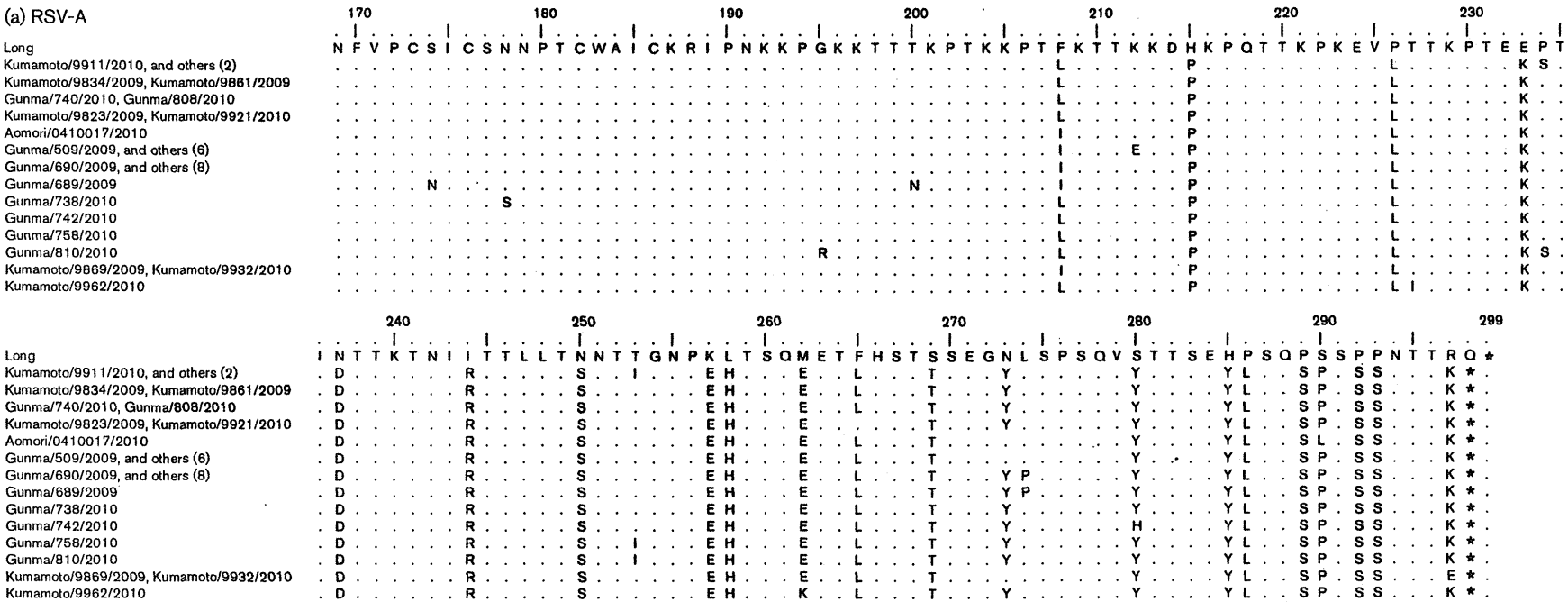

Fig. 3. Deduced amino acid alignments of the G protein in RSV-A (a) and RSV-B (b). The alignment is relative to the sequence of the prototype Long and BA4128/99B strains. The amino acids shown correspond to the Long G protein (aa 169–299) for RSV-A and to strain BA4128/99B G protein (aa 169–320) for RSV-B. Identical residues are indicated by dots, and stop codons by asterisks.

(b) RSV-B

	170										180										190										200										210										220									
BA4128/99B	N	F	V	P	C	S	I	C	G	N	N	Q	L	C	K	S	I	C	K	T	I	P	S	N	K	P	K	K	K	P	T	I	K	P	T	N	K	P	P	T	K	T	T	N	K	R	D	P	K	K	L	A	K	T	L	K	K
Gunma/433/2009, Gunma/434/2009	.	.	.	.	.	.	.	.	.	.	.	.	.	.	.	.	.	.	.	.	.	.	.	.	.	.	.	.	.	.	.	.	.	.	.	.	.	.	.	.	.	.	.	.	.	.	.	.	.	.	T	.	.	.	.	P	.	.
Gunma/470/2009, Gunma/692/2010	.	.	.	.	.	.	.	.	.	.	.	.	.	.	.	.	.	.	.	.	.	.	.	.	.	.	.	.	.	.	.	T	.	.	.	.	.	.	.	.	.	.	.	.	.	.	.	.	.	.	T	.	.	.	.	P	.	.
Gunma/775/2010, Gunma/812/2010	.	.	.	.	.	.	.	.	.	.	.	.	.	.	.	.	.	.	.	.	.	.	.	.	.	.	.	.	.	.	.	.	.	.	.	.	.	.	.	.	.	.	.	.	.	.	.	.	.	.	T	.	.	.	.	P	.	.
Gunma/777/2010	.	.	.	.	.	.	.	.	.	.	.	.	.	.	.	.	.	.	.	.	.	.	.	.	.	.	.	.	.	.	.	T	.	.	I	.	.	.	.	.	.	.	.	.	.	.	.	.	.	.	T	.	.	.	.	P	.	.
Gunma/778/2010	.	.	.	.	.	.	.	.	.	.	.	.	.	.	.	.	.	.	.	.	.	.	.	.	.	.	.	.	.	.	.	.	.	.	.	.	.	.	.	.	.	.	.	.	.	.	.	.	.	.	T	.	.	.	.	P	.	.
Gunma/780/2010	.	.	.	.	.	.	.	.	.	.	.	.	.	.	.	.	.	.	.	.	.	.	.	.	.	.	.	.	.	.	.	T	.	.	.	.	.	.	.	.	.	.	.	.	.	.	.	.	.	.	T	.	.	.	.	P	.	.
Gunma/807/2010	.	.	.	.	.	.	.	.	.	.	.	.	.	.	.	.	.	.	.	.	.	.	.	.	.	.	.	.	.	.	.	.	.	.	.	.	.	.	.	.	.	.	.	.	.	.	.	.	.	.	T	.	.	.	.	P	.	.
Gunma/830/2010,Gunma/855/2010	.	.	.	.	.	.	.	.	.	.	.	.	.	.	.	.	.	.	.	.	.	.	.	.	.	.	.	.	.	.	.	T	.	.	.	.	.	.	.	.	.	.	.	.	.	.	.	.	.	.	T	.	.	.	.	P	.	.
Gunma/831/2010	.	.	.	.	.	.	.	.	.	.	.	.	.	.	.	.	.	.	.	.	.	.	.	.	.	.	.	T	.	.	.	T	.	.	.	.	.	.	.	.	.	.	.	.	.	.	.	.	.	.	T	.	.	.	.	P	.	.
Gunma/852/2010	.	.	.	.	.	.	.	.	.	.	.	.	.	.	.	.	.	.	.	.	.	.	.	.	.	.	.	.	.	.	.	.	.	.	.	.	.	.	.	.	.	.	.	.	.	.	.	.	.	.	T	.	.	.	.	P	.	.
Kumamoto/9900/2010	.	.	.	.	.	.	.	.	.	.	.	.	.	.	.	.	.	.	.	.	.	.	.	.	.	.	.	.	.	.	.	.	.	.	.	.	.	.	.	.	.	.	.	.	.	.	.	.	.	.	T	.	.	.	.	P	.	.
Kumamoto/9941/2010	.	.	.	.	.	.	.	.	.	.	.	.	.	.	.	.	.	.	.	.	.	.	.	.	.	.	.	.	.	.	.	T	.	.	.	.	.	.	.	.	.	.	.	.	.	.	.	.	.	.	T	.	.	.	.	P	.	.

	230										240										250										260										270										280									
BA4128/99B	E	T	T	I	N	P	T	K	K	P	T	P	K	T	T	E	R	D	T	S	T	S	Q	S	T	V	L	D	T	T	S	H	T	S	K	H	T	I	S	T	S	Q	S	T	V	L	D	T	T	T	S	K	H	T	I
Gunma/433/2009, Gunma/434/2009	.	.	.	.	.	.	.	.	.	L	I	.	.	.	.	.	.	.	.	.	.	P	.	.	.	.	.	.	.	.	.	.	.	.	.	.	.	.	.	.	.	.	.	.	I	.	.	.	.	.	.	.	.	.	.	.
Gunma/470/2009, Gunma/692/2010	.	.	.	.	.	.	.	.	.	.	.	.	.	.	.	.	.	.	.	.	.	P	.	.	.	I	.	.	.	.	.	.	.	.	.	.	.	.	.	.	.	.	.	.	I	A	.	.	.	.	.	.	.	.	.	.
Gunma/775/2010, Gunma/812/2010	.	.	.	T	.	.	.	.	.	.	.	.	.	.	.	.	.	.	.	.	.	Q	.	.	.	.	.	.	.	G	.	.	.	.	.	.	.	.	.	.	.	.	.	.	I	.	.	.	A	.	.	E	.	.	V
Gunma/777/2010	.	.	.	.	.	.	.	.	.	.	.	L	.	.	.	.	.	.	.	.	.	P	.	.	.	.	.	.	.	.	.	.	.	.	.	.	.	.	.	.	.	.	.	.	.	A	.	.	.	.	.	.	.	.	.	.
Gunma/778/2010	.	.	.	.	.	.	.	.	.	.	.	.	.	.	.	.	.	.	.	.	.	P	.	.	.	.	.	.	.	.	.	.	.	.	.	.	.	L	.	.	I	A	.	.	.	.	.	.	.	.	.	.	.	.	.	.
Gunma/780/2010	.	.	.	.	.	.	.	.	.	.	.	.	.	.	.	.	.	.	.	.	.	P	.	.	.	.	.	.	.	.	.	.	.	.	.	.	.	.	.	.	I	A	.	.	.	.	.	.	.	.	.	.	.	.	T	.
Gunma/807/2010	.	.	.	.	.	.	.	.	.	.	.	.	.	.	.	.	.	.	.	.	.	P	.	.	.	.	.	.	.	.	.	.	.	.	.	.	.	L	.	.	I	A	.	.	.	.	.	.	.	.	.	.	.	.	.	.
Gunma/830/2010,Gunma/855/2010	.	.	.	.	.	.	.	.	.	.	.	L	.	.	.	.	.	.	.	.	.	P	.	.	.	.	.	.	.	.	.	.	.	.	.	.	.	.	.	.	I	A	.	.	.	.	.	.	.	.	.	.	.	.	.	.
Gunma/831/2010	.	.	.	.	.	.	.	.	.	.	.	L	.	.	.	.	.	.	.	.	.	P	.	.	.	.	.	.	.	.	.	.	.	.	.	.	.	.	.	.	I	A	.	.	.	.	.	.	.	.	.	.	.	.	.	.
Gunma/852/2010	.	.	.	.	.	.	.	.	.	.	.	.	.	.	.	.	.	.	.	.	.	P	.	.	.	.	.	.	.	.	.	.	.	.	.	.	.	.	.	.	I	A	.	.	.	.	.	.	.	.	.	.	.	.	.	.
Kumamoto/9900/2010	.	.	.	.	.	.	.	.	.	.	.	.	.	.	.	.	.	.	.	.	.	P	.	.	.	.	.	.	.	.	.	.	.	.	.	.	.	.	.	P	I	.	.	.	.	.	.	.	.	.	.	.	.	.	.	.
Kumamoto/9941/2010	.	.	.	.	.	.	.	.	.	.	.	.	.	.	.	.	.	.	.	.	.	P	.	.	.	.	.	.	.	.	.	.	.	.	.	.	.	.	.	.	I	A	.	.	.	.	.	.	.	.	.	.	.	.	.	.

	290										300										310										320				
BA4128/99B	Q	Q	Q	S	L	H	S	T	T	P	E	N	T	P	N	S	T	Q	T	P	T	A	S	E	P	S	T	S	N	S	T	Q	K	L	*	S	Y	A	*
Gunma/433/2009, Gunma/434/2009	.	.	.	.	.	Y	.	.	.	.	.	.	.	.	.	.	.	.	.	.	.	.	.	.	.	.	.	.	.	.	.	.	.	.	Q	.	.	.	.
Gunma/470/2009, Gunma/692/2010	.	.	.	.	.	Y	.	.	.	.	.	.	.	.	.	.	.	.	.	.	.	.	.	.	.	.	.	.	.	.	.	*	.	.	Q	.	.	.	.
Gunma/775/2010, Gunma/812/2010	.	.	.	.	.	.	.	.	.	.	G	.	.	.	.	.	.	.	.	.	.	.	.	.	.	.	.	.	.	.	.	*	.	.	Q	.	.	.	.
Gunma/777/2010	.	.	.	.	.	.	.	.	.	.	.	.	.	.	.	.	.	.	.	.	.	.	.	.	.	.	.	.	.	.	.	*	.	.	Q	.	.	.	.
Gunma/778/2010	.	.	.	.	.	Y	.	.	.	.	.	.	.	.	.	F	.	.	.	.	.	.	.	.	.	.	.	.	.	.	.	.	.	.	Q	.	.	.	.
Gunma/780/2010	.	.	.	.	P	Y	.	.	.	.	.	.	.	.	.	.	.	.	.	.	.	.	.	.	.	.	.	.	.	.	.	*	.	.	Q	.	.	.	.
Gunma/807/2010	.	.	.	.	.	Y	.	.	.	.	.	.	.	.	.	F	.	.	.	.	.	.	.	.	.	.	.	.	.	.	.	*	.	.	Q	.	.	.	.
Gunma/830/2010,Gunma/855/2010	.	.	.	.	.	Y	.	.	.	.	.	.	.	.	.	.	.	.	.	.	.	.	.	.	.	.	.	.	.	.	.	*	.	.	Q	.	.	.	.
Gunma/831/2010	.	.	.	.	.	Y	.	.	.	.	.	.	.	.	.	.	.	.	.	.	.	.	.	.	.	.	.	.	.	.	.	*	.	.	Q	.	.	.	.
Gunma/852/2010	.	.	.	.	.	Y	.	.	.	L	.	.	.	.	.	.	.	.	.	.	.	.	.	.	.	.	.	.	.	.	.	*	.	.	Q	.	.	.	.
Kumamoto/9900/2010	.	.	.	.	.	Y	.	.	.	.	G	.	.	.	.	.	.	.	.	.	.	.	.	.	.	.	.	.	P	.	P	.	.	P	Q	.	.	.	.
Kumamoto/9941/2010	.	.	.	.	.	Y	.	.	.	.	.	.	.	.	.	.	.	.	.	.	.	.	.	.	.	.	.	.	.	.	.	.	K	I	Q	.	.	.	.

REFERENCES

Allander, T., Tammi, M. T., Eriksson, M., Bjerkner, A., Tiveljung-Lindell, A. & Andersson, B. (2005). Cloning of a human parvovirus by molecular screening of respiratory tract samples. *Proc Natl Acad Sci U S A* **102**, 12891–12896.

Anderson, L. J., Hierholzer, J. C., Tsou, C., Hendry, R. M., Fernie, B. F., Stone, Y. & McIntosh, K. (1985). Antigenic characterization of respiratory syncytial virus strains with monoclonal antibodies. *J Infect Dis* **151**, 626–633.

Bellau-Pujol, S., Vabret, A., Legrand, L., Dina, J., Gouarin, S., Petitjean-Lecherbonnier, J., Pozzetto, B., Ginevra, C. & Freymuth, F. (2005). Development of three multiplex RT-PCR assays for the detection of 12 respiratory RNA viruses. *J Virol Methods* **126**, 53–63.

Bisno, A. L., Gerber, M. A., Gwaltney, J. M., Jr, Kaplan, E. L. & Schwartz, R. H. from the Infectious Diseases Society of America (1997). Diagnosis and management of group A streptococcal pharyngitis: a practice guideline. *Clin Infect Dis* **25**, 574–583.

Botosso, V. F., Zanotto, P. M. D. A., Ueda, M., Arruda, E., Gilio, A. E., Vieira, S. E., Stewien, K. E., Peret, T. C. T., Jamal, L. F. & other authors (2009). Positive selection results in frequent reversible amino acid replacements in the G protein gene of human respiratory syncytial virus. *PLoS Pathog* **5**, e1000254.

Cane, P. A., Matthews, D. A. & Pringle, C. R. (1991). Identification of variable domains of the attachment (G) protein of subgroup A respiratory syncytial viruses. *J Gen Virol* **72**, 2091–2096.

Echevarría, J. E., Erdman, D. D., Swierkosz, E. M., Holloway, B. P. & Anderson, L. J. (1998). Simultaneous detection and identification of human parainfluenza viruses 1, 2, and 3 from clinical samples by multiplex PCR. *J Clin Microbiol* **36**, 1388–1391.

Felsenstein, J. (1981). Evolutionary trees from DNA sequences: a maximum likelihood approach. *J Mol Evol* **17**, 368–376.

Fujitsuka, A., Tsukagoshi, H., Arakawa, M., Goto-Sugai, K., Ryo, A., Okayama, Y., Mizuta, K., Nishina, A., Yoshizumi, M. & other authors (2011). A molecular epidemiological study of respiratory viruses detected in Japanese children with acute wheezing illness. *BMC Infect Dis* **11**, 168.

Furuse, Y., Shimabukuro, K., Odagiri, T., Sawayama, R., Okada, T., Khandaker, I., Suzuki, A. & Oshitani, H. (2010). Comparison of selection pressures on the HA gene of pandemic (2009) and seasonal human and swine influenza A H1 subtype viruses. *Virology* **405**, 314–321.

Gaunt, E. R., Jansen, R. R., Poovorawan, Y., Templeton, K. E., Toms, G. L. & Simmonds, P. (2011). Molecular epidemiology and evolution of human respiratory syncytial virus and human metapneumovirus. *PLoS ONE* **6**, e17427.

Glezen, W. P., Taber, L. H., Frank, A. L. & Kasel, J. A. (1986). Risk of primary infection and reinfection with respiratory syncytial virus. *Am J Dis Child* **140**, 543–546.

Gojobori, T., Moriyama, E. N. & Kimura, M. (1990). Molecular clock of viral evolution, and the neutral theory. *Proc Natl Acad Sci U S A* **87**, 10015–10018.

Goto-Sugai, K., Tsukagoshi, H., Mizuta, K., Matsuda, S., Noda, M., Sugai, T., Saito, Y., Okabe, N., Tashiro, M. & other authors (2010). Genotyping and phylogenetic analysis of the major genes in respiratory syncytial virus isolated from infants with bronchiolitis. *Jpn J Infect Dis* **63**, 393–400.

Graham, M., Liang, B., Van Domselaar, G., Bastien, N., Beaudoin, C., Tyler, S., Kaplen, B., Landry, E., National Influenza A/H1N1pdm Genomics Study Team (NIGST) & Li, Y. (2011). Nationwide molecular surveillance of pandemic H1N1 influenza A virus genomes: Canada, 2009. *PLoS ONE* **6**, e16087.

Hall, C. B. (2004). Respiratory syncytial virus and human metapneumovirus. In *Textbook of Pediatric Infectious Diseases*, 5th edn, pp. 2315–2341. Edited by R. Feigin. Philadelphia: Saunders.

Johnson, P. R., Spriggs, M. K., Olmsted, R. A. & Collins, P. L. (1987). The G glycoprotein of human respiratory syncytial viruses of subgroups A and B: extensive sequence divergence between antigenically related proteins. *Proc Natl Acad Sci U S A* **84**, 5625–5629.

Kimura, M. (1980). A simple method for estimating evolutionary rates of base substitutions through comparative studies of nucleotide sequences. *J Mol Evol* **16**, 111–120.

Lam, W. Y., Yeung, A. C., Tang, J. W., Ip, M., Chan, E. W., Hui, M. & Chan, P. K. (2007). Rapid multiplex nested PCR for detection of respiratory viruses. *J Clin Microbiol* **45**, 3631–3640.

Leung, A. K., Kellner, J. D. & Davies, H. D. (2005). Respiratory syncytial virus bronchiolitis. *J Natl Med Assoc* **97**, 1708–1713.

Miura-Ochiai, R., Shimada, Y., Konno, T., Yamazaki, S., Aoki, K., Ohno, S., Suzuki, E. & Ishiko, H. (2007). Quantitative detection and rapid identification of human adenoviruses. *J Clin Microbiol* **45**, 958–967.

Mizuta, K., Hirata, A., Suto, A., Aoki, Y., Ahiko, T., Itagaki, T., Tsukagoshi, H., Morita, Y., Obuchi, M. & other authors (2010). Phylogenetic and cluster analysis of human rhinovirus species A (HRV-A) isolated from children with acute respiratory infections in Yamagata, Japan. *Virus Res* **147**, 265–274.

Mizuta, K., Saitoh, M., Kobayashi, M., Tsukagoshi, H., Aoki, Y., Ikeda, T., Abiko, C., Katsushima, N., Itagaki, T. & other authors (2011). Detailed genetic analysis of hemagglutinin–neuraminidase glycoprotein gene in human parainfluenza virus type 1 isolates from patients with acute respiratory infection between 2002 and 2009 in Yamagata prefecture, Japan. *Virol J* **8**, 533.

Mufson, M. A., Orvell, C., Rafnar, B. & Norrby, E. (1985). Two distinct subtypes of human respiratory syncytial virus. *J Gen Virol* **66**, 2111–2124.

Nadala, D., Bossart, W., Zucol, F., Steiner, F., Berger, C., Lips, U. & Altwegg, M. (2001). Community-acquired pneumonia in children due to *Mycoplasma pneumoniae*: diagnostic performance of a seminested 16S rDNA-PCR. *Diagn Microbiol Infect Dis* **39**, 15–19.

Nakamura, M., Itokazu, K., Taira, K., Kawaki, T., Kudaka, J., Nidaira, M., Okano, S., Koja, Y., Tamanaha, K. & other authors (2009). Genotypic and phylogenetic analysis of the *G* gene of respiratory syncytial virus isolates in Okinawa, Japan, 2008. *Jpn J Infect Dis* **62**, 326–327.

Nakauchi, M., Yasui, Y., Miyoshi, T., Minagawa, H., Tanaka, T., Tashiro, M. & Kageyama, T. (2011). One-step real-time reverse transcription-PCR assays for detecting and subtyping pandemic influenza A/H1N1 2009, seasonal influenza A/H1N1, and seasonal influenza A/H3N2 viruses. *J Virol Methods* **171**, 156–162.

Olive, D. M., Al-Mufti, S., Al-Mulla, W., Khan, M. A., Pasca, A., Stanway, G. & Al-Nakib, W. (1990). Detection and differentiation of picornaviruses in clinical samples following genomic amplification. *J Gen Virol* **71**, 2141–2147.

Palomo, C., García-Barreno, B., Peñas, C. & Melero, J. A. (1991). The G protein of human respiratory syncytial virus: significance of carbohydrate side-chains and the C-terminal end to its antigenicity. *J Gen Virol* **72**, 669–675.

Parveen, S., Sullender, W. M., Fowler, K., Lefkowitz, E. J., Kapoor, S. K. & Broor, S. (2006). Genetic variability in the G protein gene of group A and B respiratory syncytial viruses from India. *J Clin Microbiol* **44**, 3055–3064.

Pérez-Yarza, E. G., Moreno, A., Lázaro, P., Mejías, A. & Ramilo, O. (2007). The association between respiratory syncytial virus infection and the development of childhood asthma: a systematic review of the literature. *Pediatr Infect Dis J* **26**, 733–739.

Peter, L. C. & James, E. C., Jr (2006). Respiratory syncytial virus and metapneumovirus. In *Fields Virology*, pp. 1601–1646. Edited by D. M. Knipe, P. M. Howley, D. E. Griffin, M. A. Martin, R. A. Lamb, B. Roizman & S. E. Straus. Philadelphia: Lippincott Willams &Wilkins.

Pond, S. L. & Frost, S. D. (2005). Datamonkey: rapid detection of selective pressure on individual sites of codon alignments. *Bioinformatics* **21**, 2531–2533.

Rambaut, A. (2000). Estimating the rate of molecular evolution: incorporating non-contemporaneous sequences into maximum likelihood phylogenies. *Bioinformatics* **16**, 395–399.

Rebuffo-Scheer, C., Bose, M., He, J., Khaja, S., Ulatowski, M., Beck, E. T., Fan, J., Kumar, S., Nelson, M. I. & Henrickson, K. J. (2011). Whole genome sequencing and evolutionary analysis of human respiratory syncytial virus A and B from Milwaukee, WI 1998–2010. *PLoS ONE* **6**, e25468.

Reiche, J. & Schweiger, B. (2009). Genetic variability of group A human respiratory syncytial virus strains circulating in Germany from 1998 to 2007. *J Clin Microbiol* **47**, 1800–1810.

Rueda, P., Delgado, T., Portela, A., Melero, J. A. & García-Barreno, B. (1991). Premature stop codons in the G glycoprotein of human respiratory syncytial viruses resistant to neutralization by monoclonal antibodies. *J Virol* **65**, 3374–3378.

Saitou, N. & Nei, M. (1987). The neighbor-joining method: a new method for reconstructing phylogenetic trees. *Mol Biol Evol* **4**, 406–425.

Sato, M., Saito, R., Sakai, T., Sano, Y., Nishikawa, M., Sasaki, A., Shobugawa, Y., Gejyo, F. & Suzuki, H. (2005). Molecular epidemiology of respiratory syncytial virus infections among children with acute respiratory symptoms in a community over three seasons. *J Clin Microbiol* **43**, 36–40.

Shay, D. K., Holman, R. C., Newman, R. D., Liu, L. L., Stout, J. W. & Anderson, L. J. (1999). Bronchiolitis-associated hospitalizations among US children, 1980–1996. *JAMA* **282**, 1440–1446.

Sigurs, N., Bjarnason, R., Sigurbergsson, F. & Kjellman, B. (2000). Respiratory syncytial virus bronchiolitis in infancy is an important risk factor for asthma and allergy at age 7. *Am J Respir Crit Care Med* **161**, 1501–1507.

Sullender, W. M., Sun, L. & Anderson, L. J. (1993). Analysis of respiratory syncytial virus genetic variability with amplified cDNAs. *J Clin Microbiol* **31**, 1224–1231.

Takao, S., Shimozono, H., Kashiwa, H., Matsubara, K., Sakano, T., Ikeda, M., Okamoto, N., Yoshida, H., Shimazu, Y. & Fukuda, S. (2004). [The first report of an epidemic of human metapneumovirus infection in Japan: clinical and epidemiological study]. *Kansenshogaku Zasshi* **78**, 129–137 (in Japanese).

Tripp, R. A., Jones, L. P., Haynes, L. M., Zheng, H., Murphy, P. M. & Anderson, L. J. (2001). CX3C chemokine mimicry by respiratory syncytial virus G glycoprotein. *Nat Immunol* **2**, 732–738.

Vardas, E., Blaauw, D. & McAnerney, J. (1999). The epidemiology of respiratory syncytial virus (RSV) infections in South African children. *S Afr Med J* **89**, 1079–1084.

Woelk, C. H. & Holmes, E. C. (2001). Variable immune-driven natural selection in the attachment (G) glycoprotein of respiratory syncytial virus (RSV). *J Mol Evol* **52**, 182–192.

Yeo, D. S.-Y., Seah, S. G.-K., Chew, J. S.-W., Lim, E. A.-S., Liaw, J. C.-W., Loh, J.-P. & Tan, B.-H. (2007). Molecular identification of coxsackievirus A24 variant, isolated from an outbreak of acute hemorrhagic conjunctivitis in Singapore in 2005. *Arch Virol* **152**, 2005–2016.

Yorita, K. L., Holman, R. C., Steiner, C. A., Effler, P. V., Miyamura, J., Forbes, S., Anderson, L. J. & Balaraman, V. (2007). Severe bronchiolitis and respiratory syncytial virus among young children in Hawaii. *Pediatr Infect Dis J* **26**, 1081–1088.

Zhang, W. D. & Evans, D. H. (1991). Detection and identification of human influenza viruses by the polymerase chain reaction. *J Virol Methods* **33**, 165–189.

Zlateva, K. T., Lemey, P., Vandamme, A. M. & Van Ranst, M. (2004). Molecular evolution and circulation patterns of human respiratory syncytial virus subgroup A: positively selected sites in the attachment G glycoprotein. *J Virol* **78**, 4675–4683.

Zlateva, K. T., Lemey, P., Moës, E., Vandamme, A. M. & Van Ranst, M. (2005). Genetic variability and molecular evolution of the human respiratory syncytial virus subgroup B attachment G protein. *J Virol* **79**, 9157–9167.

THE JOURNAL OF BIOLOGICAL CHEMISTRY VOL. 286, NO. 13, pp. 11593–11603, April 1, 2011

A Distinct Role for Pin1 in the Induction and Maintenance of Pluripotency*

Received for publication, September 23, 2010, and in revised form, February 3, 2011 Published, JBC Papers in Press, February 4, 2011, DOI 10.1074/jbc.M110.187989

Mayuko Nishi,[a] Hidenori Akutsu,[b] Shinji Masui,[c] Asami Kondo,[a] Yoji Nagashima,[d] Hirokazu Kimura,[e] Kilian Perrem,[f] Yasushi Shigeri,[g] Masashi Toyoda,[b] Akiko Okayama,[h] Hisashi Hirano,[h] Akihiro Umezawa,[b] Naoki Yamamoto,[i] Sam W. Lee,[j] and Akihide Ryo[a1]

From the Departments of [a]Microbiology, [d]Pathology, and [h]Supramolecular Biology, Yokohama City University School of Medicine, Yokohama 236-0004, Japan, the [b]Department of Reproductive Biology, National Research Institute for Child Health and Development, Tokyo 157-8535, Japan, the [c]Department of Regenerative Medicine, Research Institute, International Medical Center of Japan, Tokyo 162-8655, Japan, the [e]Infectious Disease Surveillance Center, National Institute of Infectious Diseases, Tokyo 208-0011, Japan, the [f]Commonwealth Scientific and Industrial Research Organization, P.O. Box 225, Dickson, Australian Capital Territory 2602, Australia, the [g]National Institute of Advanced Industrial Science and Technology, Osaka 563-8577, Japan, the [i]Department of Microbiology, National University of Singapore, 117597 Singapore, and the [j]Cutaneous Biology Research Center, Massachusetts General Hospital and Harvard Medical School, Charlestown, Massachusetts 02129

The prominent characteristics of pluripotent stem cells are their unique capacity to self-renew and pluripotency. Although pluripotent stem cell proliferation is maintained by specific intracellular phosphorylation signaling events, it has not been well characterized how the resulting phosphorylated proteins are subsequently regulated. We here report that the peptidyl-prolyl isomerase Pin1 is indispensable for the self-renewal and maintenance of pluripotent stem cells via the regulation of phosphorylated Oct4 and other substrates. Pin1 expression was found to be up-regulated upon the induction of induced pluripotent stem (iPS) cells, and the forced expression of Pin1 with defined reprogramming factors was observed to further enhance the frequency of iPS cell generation. The inhibition of Pin1 activity significantly suppressed colony formation and induced the aberrant differentiation of human iPS cells as well as murine ES cells. We further found that Pin1 interacts with the phosphorylated Ser[12]-Pro motif of Oct4 and that this in turn facilitates the stability and transcriptional activity functions of Oct4. Our current findings thus uncover an atypical role for Pin1 as a putative regulator of the induction and maintenance of pluripotency via the control of phosphorylation signaling. These data suggest that the manipulation of Pin1 function could be a potential strategy for the stable induction and proliferation of human iPS cells.

Stem cells are characterized by their ability to self-renew through mitotic cell division and to differentiate into a diverse range of specialized cell types (1, 2). Human pluripotent stem cell proliferation is maintained through the action of several transcription factors including Oct4 (octamer 4), SOX2, Klf-4, Nanog, and c-Myc, which perform reprogramming functions under the stimulatory effects of stem cell-specific growth factors, including basic fibroblast growth factor (3–5). Basic fibroblast growth factor signaling has been shown to be essential for pluripotency as its depletion from cell culture media leads to aberrant cell differentiation and cell death (6, 7). Fibroblast growth factors produce mitogenic effects in targeted cells via signaling through cell surface receptor tyrosine kinases (8). These kinases can initiate intracellular signaling in cells, which is transmitted and diffused by tyrosine phosphorylation of the assembled proteins and of cellular substrates, including protein kinases with specificity for serine/threonine residues (8, 9). Although this intracellular phosphorylation signaling might indeed contribute to the self-renewal and pluripotency of stem cells (10, 11), it has not yet been fully determined how these phosphorylated proteins are further regulated.

Protein phosphorylation is a fundamental mode of intracellular signal transduction in a variety of key cellular processes such as cell proliferation, differentiation, and morphogenesis (12). A pivotal signaling mechanism that controls the function of phosphorylated proteins is the *cis-trans* isomerization of phosphorylated Ser/Thr-Pro motifs by the peptidylprolyl isomerase Pin1 (13, 14). This modification regulates multiple intracellular signaling pathways, including ErbB2/Ras, Wnt/β-catenin, and NF-κB, and thus plays an important role in the etiology of several human diseases (15–18). These include various cancers, Alzheimer disease, and immune disorders (14, 17, 18). However, the role of Pin1 in regulating the properties of pluripotent stem cells has not been adequately investigated to date.

In our current study, we investigated the role of Pin1 in the self-renewal and stemness of pluripotent stem cells. We reveal that Pin1 is induced upon cellular reprogramming and that its blockade significantly inhibits the self-renewal and maintenance of human iPS[2] cells in addition to murine ES cells. We find also that Pin1 can interact with phosphorylated Oct4 at the

* This work was supported in part by grants from the Takeda Science Foundation, Uehara Memorial Foundation, and Kanagawa Nanbyo Foundation (to A. R.).

[1] To whom correspondence should be addressed: Dept. of Microbiology, Yokohama City University School of Medicine, 3-9 Fuku-ura, Kanazawa-ku, Yokohama 236-0004, Japan. Tel.: 81-45-787-2602; Fax: 81-45-787-2851; E-mail: aryo@yokohama-cu.ac.jp.

[2] The abbreviations used are: iPS, induced pluripotent stem; AP, alkaline phosphatase; dnPin1, dominant-negative Pin1; 4F, four reprogramming factors; DMSO, dimethyl sulfoxide; SUMO, small ubiquitin-like modifier; Oct4, Octamer 4.

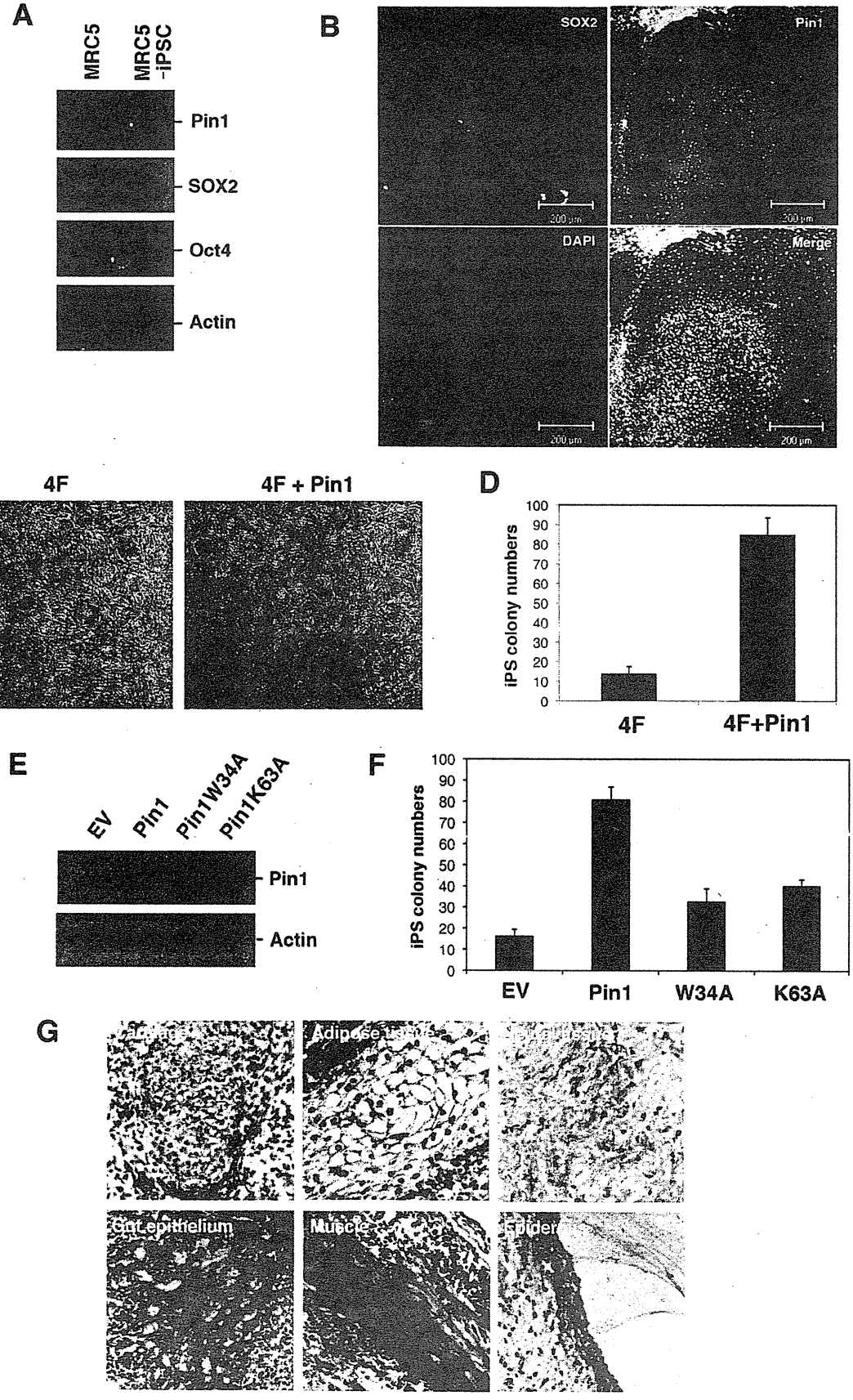

Ser[12]-Pro motif in this protein. This enhances the stability and hence the transcriptional activity of Oct4. Our present data thus suggest that Pin1 is indeed a putative regulator of the self-renewal and proliferation of pluripotent stem cells.

EXPERIMENTAL PROCEDURES

Colony Formation Analysis—Human iPS cells were obtained from the RIKEN BioResource Center (clone no. 201B7) (19). Cells were cultured in human embryonic stem cell culture medium (KnockOut Dulbecco's modified Eagle's medium (Invitrogen)) supplemented with 20% KnockOut SR (Invitrogen), 1% GlutaMAX (Invitrogen), 100 μM nonessential amino acids (Invitrogen), 50 μM β-mercaptoethanol, and 10 ng/ml basic fibroblast growth factor). Murine ES cells were cultured in human embryonic stem cell culture medium (KnockOut Dulbecco's modified Eagle's medium supplemented with 15% KnockOut SR, 1% GlutaMAX (Invitrogen), 100 μM nonessential amino acids, 50 μM β-mercaptoethanol, and 1000 units/ml recombinant human leukemia inhibitory factor) (20). Colony formation was scored by counting the number of alkaline phosphatase (AP)-positive colonies as described previously (21). The number of cells per colony was determined by manually counting the number of DAPI-stained cells (21).

Cell Reprogramming—MRC5 fibroblasts were transduced with retroviral vectors encoding reprogramming factors as described previously (19). Briefly, the retroviral vector plasmids pMXs-hOct4, pMXs-hSOX2, pMXs-hKLF4, pMXs-hcMYC (Addgene), and pVSV-G were introduced into Plat-E cells using Effectene transfection reagent (Qiagen). After 48 h, virus-containing supernatants were passed through a 0.45-μm filter and supplemented with 10 μg/ml hexadimethrine bromide (polybrene). Cells were seeded at 6×10^5 cells per 60 mm dish at 24 h before incubation in the virus/polybrene-containing supernatants for 16 h. After 6 days, cells were plated on irradiated mouse embryonic fibroblasts, and culture medium was replaced with the hESC culture medium 24 h later. Cells were maintained at 37 °C and 5% CO_2 for 30 days.

Construction of Expression Vectors—Oct4 cDNA was subcloned into pcDNA3-HA expression vector (Invitrogen). Expression constructs of Oct4 were as follows: pcDNA-HA-Oct4 wild-type, amino acids 1–360; pcDNA-HA-Oct4 ΔC, amino acids 1–297; pcDNA-HA-Oct4 ΔN1, amino acids 138–360; pcDNA-HA-Oct4 ΔN2, amino acids 113–360; and pcDNA-HA-Oct4 ΔN3, amino acids 34–360. pcDNA-HA-Oct4-S12A was generated by KOD-Plus Mutagenesis Kit (Toyobo, Osaka, Japan) according to the manufacturer's instructions. The primers were 5′-CGCCCCCTCCAGGTGGT-3′ (forward) and 5′-CGAAGGCAAAATCTGAAGCC-3′ (reverse).

Gene Reporter Assay—A pGL3-fgf4 reporter plasmid containing an Oct-SOX binding cassette and the firefly luciferase gene was transfected with pRL-CMV (22). The −2601/+1 (nucleotide positions indicated with respect to the +1 translation start site) genomic fragment of the Oct4 promoter upstream region was amplified by PCR from human lymphocyte genomic DNA and cloned into the KpnI/HindIII sites of the pGL4-basic reporter plasmid (Promega, Madison, WI) as described previously (23). The primer sets were as follows: 5′-CCTGGTACCAGGATGGCAAGCTGAGAAACACTG-3′ and 5′-TCGCAAGCTTGCGAAGGGACTACTCAAC-3′. Cells were transfected with reporter plasmid vectors using Effectene (Qiagen) or Xfect Stem (Clontech). One day after transfection, the cells were resuspended in passive lysis buffer (Promega) and incubated for 15 min at room temperature. Luciferase activities were measured with a Dual-Luciferase reporter assay system (Promega) in accordance with the manufacturer's instructions.

GST Pulldown Assay and Immunoprecipitation Analysis—Cells were lysed with GST pulldown buffer (50 mM HEPES (pH 7.4), 150 mM NaCl, 10% glycerol, 1% Triton X-100, 1.5 mM $MgCl_2$, 1 mM EGTA, 100 mM NaF, 1 mM Na_3VO_4, 1 mM DTT, 5 μg/ml leupeptin, 1 μg/ml pepstatin, and 0.2 mM PMSF) and incubated with 30 μl of glutathione-agarose beads containing either GST-Pin1 or GST at 4 °C for 2 h. The precipitated proteins were then washed three times with lysis buffer and subjected to SDS-PAGE. For immunoprecipitation, cells were lysed with Nonidet P-40 lysis buffer (10 mM Tris HCl (pH 7.4), 100 mM NaCl, 0.5% Nonidet P-40, 1 mM Na_3VO_4, 100 mM NaF, 5 μg/ml leupeptin, 1 μg/ml pepstatin, and 0.2 mM PMSF). Cell lysates were incubated for 1 h with protein A/G-Sepharose·nonimmunized IgG complexes. Supernatant fractions were recovered and immunoprecipitated with 5 μg of anti-Myc antibody and 30 μl protein A/G-Sepharose. After washing three times with lysis buffer, the pellets were analyzed by SDS-PAGE.

Proteomics Analysis—Human iPS cell lysates were processed for immunoprecipitation with a monoclonal anti-Pin1 antibody (clone 257417, R&D Systems) at 4 °C for 3 h followed by SDS-PAGE. Gel lanes corresponding to the region from ~30 to 150 kDa were systematically excised, and the pieces were reduced, alkylated, and trypsinized. Peptides were analyzed by the linear ion trap Orbitrap hybrid mass spectrometer (Thermo Scientific). Protein identification was performed by peptide

FIGURE 1. **Pin1 is preferentially expressed in human iPS cells.** *A*, immunoblotting analysis of Oct4, SOX2, and Pin1 in MRC5 and MRC5-derived iPS cells. Actin was used as a loading control. *iPSC*, induced pluripotent stem cells; *EV*, empty vector. *B*, immunofluorescent analysis of Pin1 and SOX2 in human iPS cells. Representative images of phase-contrast microscopy and fluorescent immunocytochemistry for SOX2 (*red*) and Pin1 (*green*) are shown. Nuclei are indicated by DAPI staining (*blue*). Note that Pin1 is highly expressed in SOX2-positive pluripotent stem cells. *C* and *D*, Pin1 expression enhances 4F (Oct4, SOX2, Klf4, and c-Myc)-induced iPS cell induction. MRC5 fibroblasts were infected with retrovirus vectors encoding 4F and co-infected with those encoding either empty vector or Pin1. A representative picture of colony formations stained with AP is shown (*C*). The numbers of AP-positive colonies were scored in three independent experiments (*D*). Note that the co-introduction of Pin1 with 4F increases the frequency of iPS colony formation. *E* and *F*, MRC5 fibroblasts were infected with retrovirus vectors encoding 4F and co-infected with those encoding empty vector, HA-tagged wild-type Pin1, or its W34A or K63A mutants. The expression levels of HA-Pin1 or its mutants in infected MRC5 cells were analyzed by immunoblotting analysis with anti-HA antibody (*E*). The number of AP-positive colonies was scored in three independent experiments (*F*). *G*, teratoma tissue derived from human iPS cells induced by 4F and Pin1. iPS cells were transplanted subcutaneously into immunodeficient mice (2×10^6/mouse). Representative images of hematoxylin and eosin stained tumor with light microscope (200×) are shown.

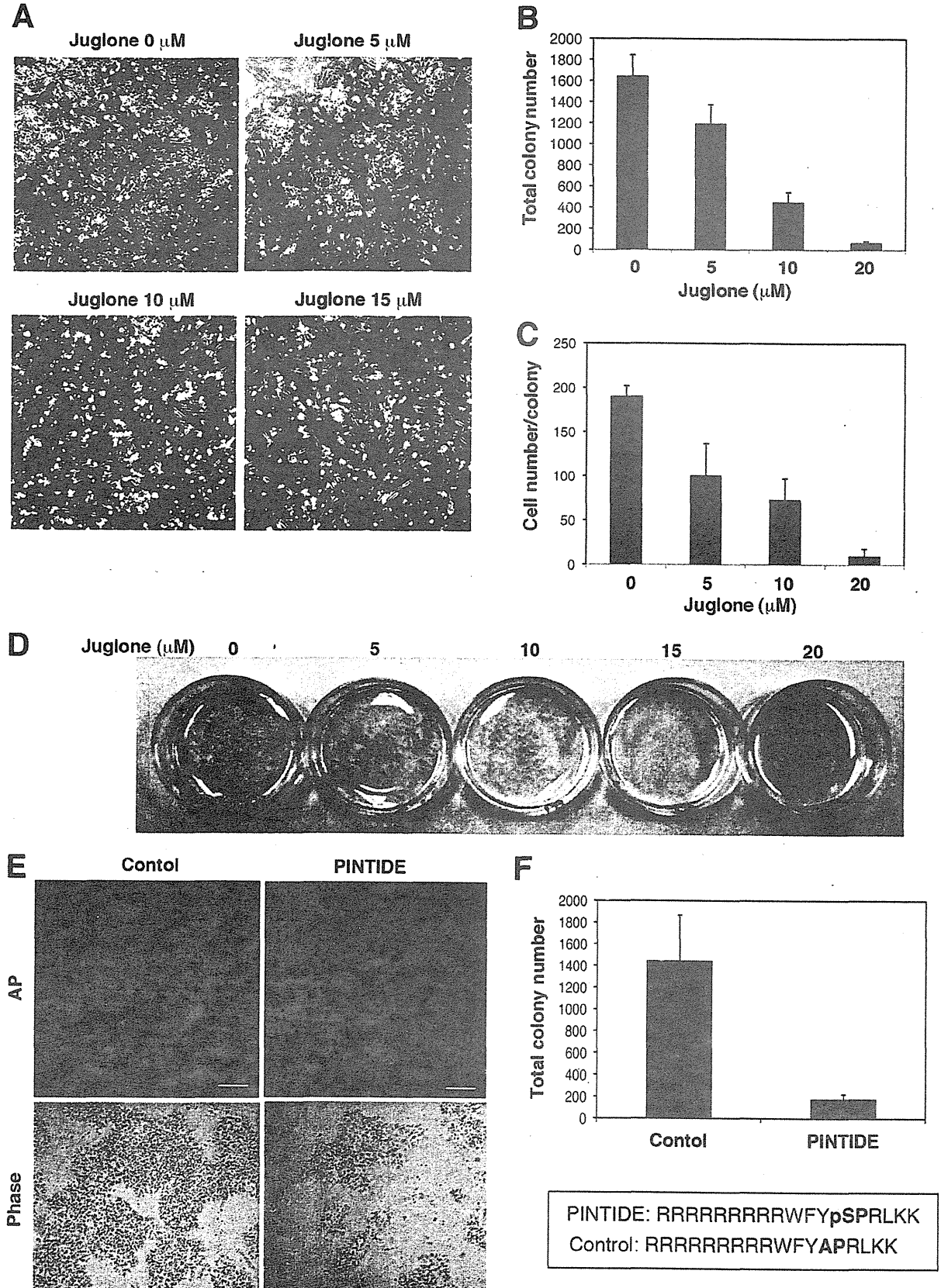

mass fingerprinting with the Mascot and Aldente search algorithms.

Quantitative Real-time PCR—Total RNA was extracted with TRIzol reagent (Invitrogen) according to the manufacturer's protocol. cDNA was synthesized using a cDNA synthesis kit (Toyobo, Osaka, Japan) and subjected to RT-PCR analysis with the SYBR Premix Ex gent Kit TaqII (Takara Bio, Shiga, Japan) using an Applied Biosystems 7300 real-time PCR System. The primer sets used were as follows: mOct4, 5′-CGTGTGAGGTGGAGTCTGGAGACC-3′ and 5′-ACTCGAACCACATCCTTCTCTAGCC-3′; mGAPDH, 5′-CCATGGAGAAGGCTGGGG-3′ and 5′-CAAAGTTGTCATGGATGACC-3′.

Teratoma Formation—Cells were harvested using accutase, collected into tubes, and centrifuged. The pellets were then suspended in human ESC culture medium. Fox Chase severe combined immunodeficiency mice (CREA, Tokyo, Japan) were injected with 2×10^6 cells mixed with an equal volume of Matrigel (BD Biosciences). Frozen tumor tissues embedded in optimum cutting temperature compound were sliced by cryosectioning and stained with hematoxylin and eosin.

RESULTS

Pin1 Is Induced upon Cellular Reprogramming and Enhances Generation of iPS Cells—To examine the role of Pin1 in cellular reprogramming and pluripotency, we initially investigated the expression levels of this prolyl isomerase in human iPS cells. Pin1 was found to be significantly induced upon the generation of iPS cells derived from MRC5 human fibroblasts (Fig. 1*A*). Immunofluorescent analysis further revealed that Pin1 is selectively expressed in SOX2-positive pluripotent stem cells, whereas its expression was found to be significantly suppressed in the surrounding SOX2-negative differentiated cells (Fig. 1*B*). These results indicate that Pin1 is preferentially expressed in reprogramming stem cells.

We next evaluated whether Pin1 affects the reprogramming of somatic cells into iPS cells. The co-infection of a Pin1-encoding retrovirus vector with those encoding four defined reprogramming factors (4F; SOX2, Oct4, Klf-4, and c-Myc) (24) notably boosted the generation of AP-positive iPS cell colonies compared with an induction of human fibroblast MRC5 cells with only four iPS factors (Fig. 1, *C* and *D*). We next performed a parallel experiment using either a WW-domain (binding domain) mutant (W34A) or a peptidyl prolyl isomerase-domain (catalytic domain) mutant (K63A) of Pin1. We confirmed the equivalent expression of each of these mutants and wild-type Pin1 (Fig. 1*E*). Neither of these mutants could boost iPS cell colony formation to the level seen with wild-type Pin1 (Fig. 1*F*), indicating that both the WW and PPIase domains are required for this function.

To test pluripotency *in vivo*, we transplanted 4F plus Pin1-introduced iPS cells subcutaneously into the dorsal flanks of immunodeficient mice. Nine weeks after injection, we observed teratoma formation composed of various tissues including gut-like epithelial tissues (endoderm), striated muscle (mesoderm), cartilage (mesoderm), neural tissues (ectoderm), and epidermal tissues (ectoderm) (Fig. 1*G*). These results indicate that the expression of Pin1 with defined reprogramming factors accelerates the frequency of iPS cell generation.

Pin1 Is Required for Pluripotent Stem Cell Self-renewal and Colony Formation—We next addressed whether Pin1 indeed plays any roles in the self-renewal of human iPS cells. iPS cells were dissociated with accutase and then plated at a clonal density in the presence of several concentrations of the selective Pin1 inhibitor juglone (5-hydroxy-1,4-naphthoquinone) (25, 26). The blockade of Pin1 by juglone considerably reduced both the numbers and size of the colonies in a dose-dependent manner (Fig. 2, *A–C*). It was notable also that the concentration of juglone used did not illicit nonspecific toxic effects in the feeder mouse embryonic fibroblast cells (Fig. 2*A* and data not shown). The effect of Pin1 inhibition upon colony formation was also confirmed in feeder-free cultures of human iPS cells by AP staining (Fig. 2*D*). Moreover, treatment with the Pin1 inhibitory phosphopeptide PINTIDE (27), but not a nonphosphorylated control peptide, significantly reduced the colony formation of human iPS cells (Fig. 2, *E* and *F*).

We next investigated the effects of Pin1 inhibition upon colony formation in murine ES cells. The blockade of Pin1 by juglone significantly reduced the colony numbers in two different murine ES cell types, BDF2 and R1 (Fig. 3*A*). The adenovirus-mediated transduction of a GFP-fused dominant-negative Pin1 (GFP-dnPin1) (28), but not a GFP control, significantly suppressed colony formation in murine ES (R1) cells manifesting as a considerable reduction in both the numbers and colony size of the murine ES cells (Fig. 3, *B–D*). These results together demonstrate that Pin1 is indispensable for the self-renewal and proliferation of pluripotent stem cells.

Pin1 Functions in Maintenance of Pluripotency—We next asked whether Pin1 has any roles in the maintenance of pluripotency in stem cells. Human iPS cells were dissociated and then cultured for 5 days to form colonies. When human iPS cells are cultured in hES medium supplemented with basic fibroblast growth factor, the overwhelming majority of the cells in the colonies are undifferentiated (Fig. 4*A*). However, treatment with juglone resulted in aberrant cell differentiation resulting in a "mosaic pattern" of iPS cell colonies following AP staining (Fig. 4*A*). Similarly, the adenovirus-mediated transduction of GFP-dnPin1, but not a GFP control, prominently reduced the number of AP-positive undifferentiated cells in murine ES cell colonies (Fig. 4*B*). These results together indicate that Pin1 can sustain pluripotent stem cells in an undifferentiated state in addition to the enhancement of self-renewal.

FIGURE 2. **Defective self-renewal of human iPS cells caused by Pin1 inhibition.** *A–C*, human iPS cells were dissociated with accutase and then plated on a feeder cell layer at a clonal density in the presence of the indicated concentrations of juglone for 3 days. Colony formation was analyzed by phase-contrast microscopy (*A*). The number of colonies was counted at 3 days after treatment (*B*). The number of cells per colony was determined by manually counting the DAPI-stained cells (*C*). Data are the mean ± S.E. *D*, human iPS cells were plated at a clonal density on the feeder-free culture in the presence of the indicated concentrations of juglone followed by AP staining. *E* and *F*, human iPS cells were dissociated with accutase and then plated on feeder-free dishes at a clonal density in the presence of 50 μg/ml of the Pin1 inhibitory phosphopeptide PINTIDE (RRRRRRRRRWFYpSPRLKK) or a nonphosphorylated control peptide (RRRRRRRRRWFYAPRLKK) for 48 h (*E*). AP-positive colony numbers were scored (*F*). Data are the mean ± S.E. *Scale bar*, 50 μm.

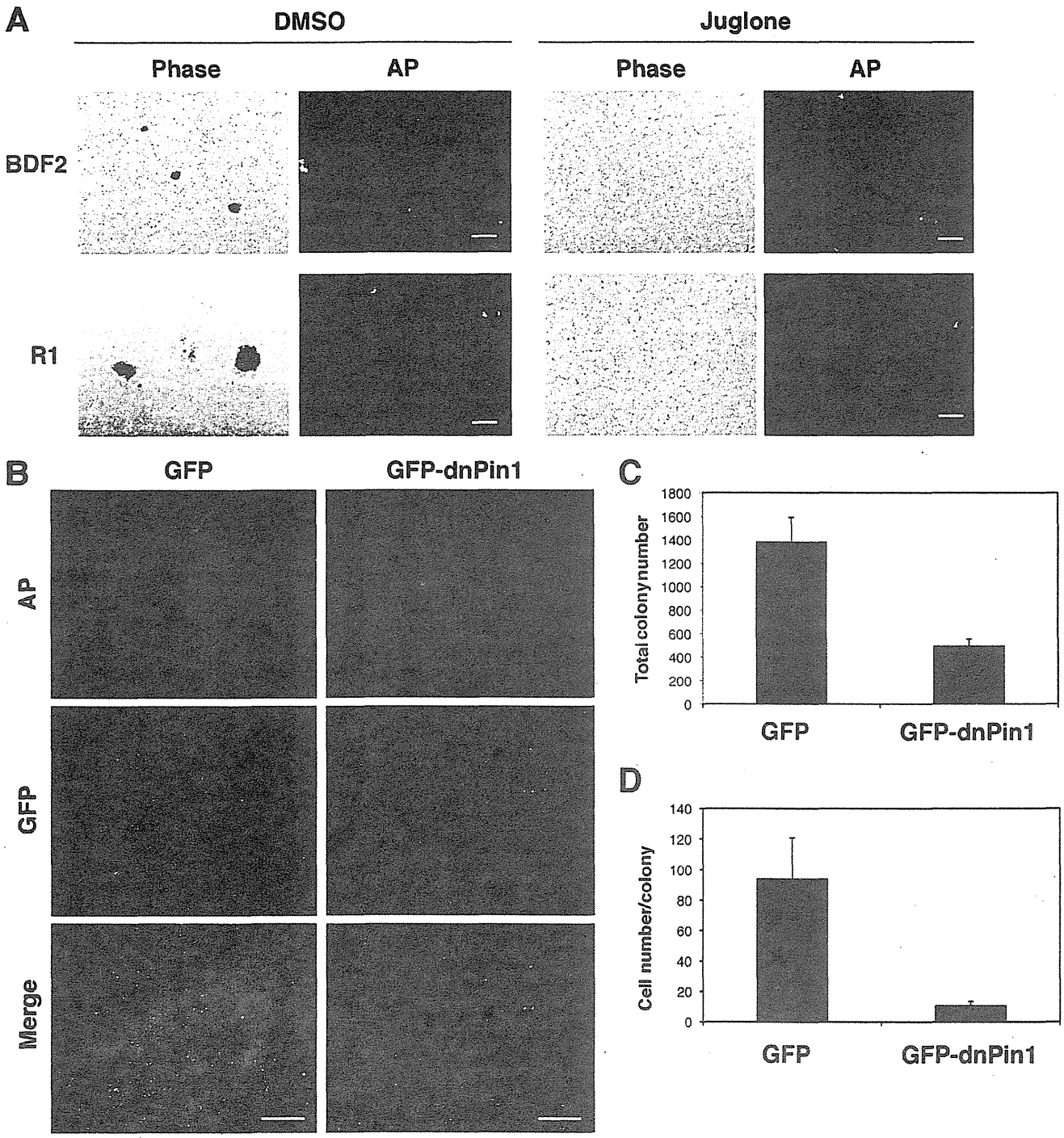

FIGURE 3. **Pin1 inhibition suppresses colony formation in murine ES cells.** *A*, two different murine ES cell types (BDF2 and R1) were plated on gelatin-coated dishes and treated with either DMSO or juglone (10 μM). Colonies were stained with AP (*red*). *Scale bar*, 200 μm. *B–D*, murine ES cells (R1) were infected with an adenovirus vector encoding either GFP or GFP-dnPin1 (3000 viral particles/cell). The cells were then stained with AP (*red*) and DAPI and analyzed by immunofluorescent microscopy (*B*). *Scale bar*, 200 μm. The total colony number (*C*) and the number of cells per colony (*D*) were then determined. Data are the mean ± S.E.

Identification of Pin1 Binding Proteins in Human iPS Cells—Our initial data indicated that Pin1 could enhance the function of reprogramming factors during the induction and maintenance of pluripotency. We next identified the substrates targeted by Pin1 in human iPS cells. Using a monoclonal Pin1 antibody, we co-immunoprecipitated proteins from human iPS cell lysates treated with a phosphatase inhibitor mixture. These isolated immune complexes were then boiled and resolved by one-dimensional SDS-PAGE, and the proteins were visualized using silver staining. Continuous regions of the gel corresponding to proteins of ~30 to 150 kDa in size were systematically excised (Fig. 5*A*), digested with trypsin, and analyzed in a linear

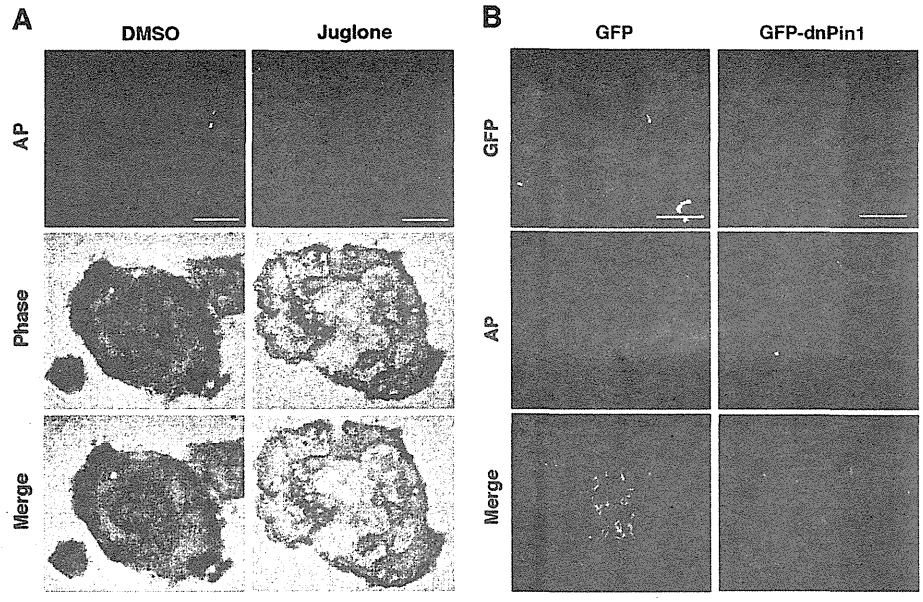

FIGURE 4. **Pin1 inhibition leads to the aberrant cell differentiation of human iPS cells.** *A*, human iPS cells were cultured for 5 days before forming colonies and then treated with either DMSO or juglone (10 μM) for 3 days. The cells were then stained with AP (*red*). Representative images of phase-contrast microscopy and fluorescent immunocytochemistry are shown. *Scale bar*, 200 μm. *B*, mouse ES cells were cultured for 2 days before forming colonies and then infected with an adenovirus vector encoding either GFP or GFP-dnPin1 (3000 viral particles/cell). After 48 h, the cells were then stained with AP (*red*) and DAPI (*blue*) and analyzed by immunofluorescent microscopy. *Scale bar*, 50 μm.

ion trap (LTQ) Orbitrap hybrid mass spectrometer. Peptide mass fingerprinting with the Mascot and Aldente search algorithms subsequently identified 23 Pin1 interacting proteins in human iPS cells (Fig. 5*B*). Notably, these Pin1-binding proteins included the pluripotent transcription factor Oct4. Because Oct4 has been shown to be a master regulator of pluripotency (29), we decided to further analyze the Oct4-Pin1 interaction.

Pin1 Binds and Regulates Protein Stability of Oct4—To further characterize the Oct4-Pin1 interaction, a GST pulldown analysis was initially performed. We found that recombinant GST-Pin1, but not GST alone, binds Oct4. This association was completely abolished by pretreatment of the cell lysates with calf intestine alkaline phosphatase (Fig. 6*A*), indicating that Pin1 binds phosphorylated Oct4. Immunofluorescence analysis further demonstrated that Pin1 co-localizes with Oct4 in the nuclei of iPS cells (Fig. 6*B*). Pin1 has been shown to regulate the stability of its substrate proteins upon binding (17), and we thus addressed whether this was the case for Oct4. Cycloheximide analysis using HeLa cells transfected with Oct4 alone or co-transfected with Oct4 and Pin1 revealed that the protein half-life of Oct4 is significantly enhanced in cells co-expressing Pin1 (Fig. 6*C*). Moreover, immunoprecipitation analysis with cells co-transfected with Oct4 and Myc-tagged ubiquitin, with or without Pin1 co-transfection, further revealed that Pin1 overexpression significantly reduces the polyubiquitination of the Oct4 protein (Fig. 6*D*). Consistently, the Oct4 protein expression level was significantly reduced in human iPS cells treated with juglone as compared with control cells (Fig. 6*E*). These results together confirm that Pin1 enhances the protein stability of Oct4 by suppressing ubiquitin proteasome-mediated proteolysis.

We next investigated the gene expression profile of Oct4 during the inhibition of Pin1. Murine ES cells were transfected with pGL4-Oct4-2601 promoter (harboring a genomic fragment of the Oct4 gene 5′-upstream region) and treated or not with juglone. Pin1 inhibition by juglone did not affect the transcriptional activity of the Oct4 promoter (Fig. 6*F*). Consistently, the results of parallel quantitative RT-PCR analysis demonstrated that the Oct4 mRNA level was not significantly altered by Pin1 inhibition (Fig. 6*G*), whereas the Oct4 protein level was significantly reduced by juglone treatment, as revealed by immunoblot analysis (Fig. 6*H*). These results together indicate that Pin1 regulates the protein stability of Oct4 but not Oct4 transcription.

We next addressed whether Pin1 enhances the transcriptional activity of the Oct4 protein. A luciferase reporter assay using the Oct-Sox enhancer region derived from the FGF4 gene was performed in HeLa cells co-transfected with Oct4, SOX2 or Pin1. Although the sole expression of Pin1 had no significant effects, the co-expression of Oct4 and Pin1 produced a significant increase in reporter activity in a dose-dependent fashion (Fig. 6*I*). This indicated that Pin1 promotes Oct4-mediated transcriptional activation. We performed a parallel experiment using the W34A and K63A Pin1 mutants. Neither of these mutants up-regulated the transcriptional activity of Oct4 to the levels seen with wild-type Pin1 (Fig. 6*J*), indicating that both the WW and PPIase domains are required for this function.

Pin1 Interacts with Ser^{12}*-Pro motif of Oct4*—To identify the specific Pin1 binding site within the Oct4 protein, we generated several Oct4 deletion mutants and performed GST-pulldown analysis. These experiments revealed that a C-terminal Oct4 deletion mutant (representing amino acids 1–297) could still bind Pin1, but that three extended N-terminal deletion mutants (amino acids 138–360, 113–360, or 34–360) failed to do so (Fig. 7*A*). These data indicate that Pin1 binds to Oct4 in the region between amino acids 1 and 34. Previous reports have indicated

A

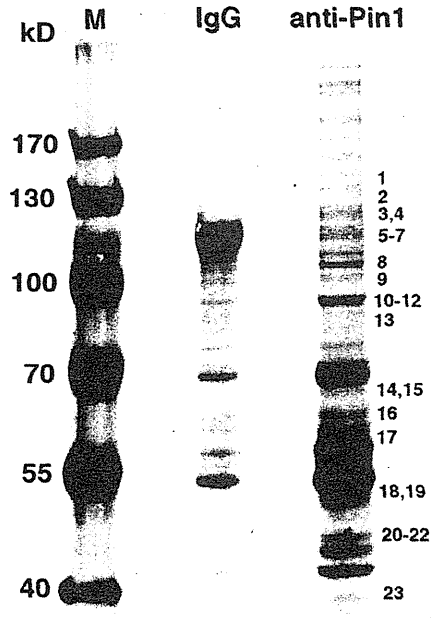

B

No.	Accession No.	Gene description	Predicted size
1	ADCY5_HUMAN	Adenylate cyclase type 5	138818
2	CCD40_HUMAN	Coiled-coil domain-containing protein 40	130033
3	PK3CA_HUMAN	Phosphatidylinositol-4,5-bisphosphate 3-kinase catalytic subunit alpha	124203
4	ZEB1_HUMAN	Zinc finger E-box-binding homeobox 1	123997
5	VINC_HUMAN	Vinculin	123722
6	RADIL_HUMAN	Ras-associating and dilute domain-containing protein	117351
7	UBP2L_HUMAN	Ubiquitin-associated protein 2-like	114465
8	DSG1_HUMAN	Desmoglein-1	113644
9	ENPP3_HUMAN	Ectonucleotide pyrophosphatase/phosphodiesterase family member 3	100059
10	ZN337_HUMAN	Zinc finger protein 337	86819
11	NASP_HUMAN	Nuclear autoantigenic sperm protein	85186
12	ZY11B_HUMAN	Protein zyg-11 homolog B	83921
13	MPEG1_HUMAN	Macrophage-expressed gene 1 protein	78587
14	FA13C_HUMAN	Protein FAM13C	65687
15	VPS45_HUMAN	Vacuolar protein sorting-associated protein 45	65036
16	ANR53_HUMAN	Ankyrin repeat domain-containing protein 53	59493
17	RPA34_HUMAN	DNA-directed RNA polymerase I subunit RPA34	54951
18	VIME_HUMAN	Vimentin	53619
19	KCAB1_HUMAN	Voltage-gated potassium channel subunit beta-1	46534
20	PRS8_HUMAN	26S protease regulatory subunit 8	45597
21	FKBP8_HUMAN	Peptidyl-prolyl cis-trans isomerase FKBP8	44534
22	PO5F1_HUMAN	POU domain, class 5, transcription factor 1 (OCT4)	38571
23	THAP1_HUMAN	THAP domain-containing protein 1	24928

FIGURE 5. **Identification of Pin1-binding proteins in human iPS cells.** *A* and *B*, lysates of human iPS cells were subjected to immunoprecipitation with either non-immunized control mouse IgG (IgG) or mouse anti-Pin1 monoclonal antibodies. Proteins bound to protein A/G-agarose beads were isolated, resolved by SDS-PAGE, and detected by silver staining (*A*). *M* indicates protein marker. Excised gel bands were digested with trypsin and analyzed on a linear ion trap (LTQ) Orbitrap hybrid mass spectrometer followed by peptide mass fingerprinting with the Mascot and Aldente search algorithms (*B*).

that Pin1 can bind only phosphorylated Ser/Thr-Pro motifs (17, 27) of which only one (Ser^{12}-Pro) exists between residues 1 and 34 in the Oct4 protein. Interestingly, this motif is conserved between various species including human, mouse, rat, and rabbit (Fig. 7*B*). We generated an Oct4 site-directed mutant at this site by substituting serine 12 for alanine (S12A). GST pulldown analysis subsequently revealed that Pin1 binds wild-type Oct4, but not its S12A mutant (Fig. 7*C*). These results confirm that Pin1 indeed bind the phosphorylated Ser^{12}-Pro motif of Oct4.

To further examine the functional interactions between Pin1 and Oct4 on this site, we next investigated the nature of the S12A mutant in terms of its protein expression in the presence of Pin1. HeLa cells were transfected with either wild-type Oct4 or its S12A mutant and co-transfected with Pin1. This was followed by immunoblotting analysis. We found that Pin1 increased the expression levels of wild-type Oct4, but not the S12A mutant (Fig. 7*D*).

DISCUSSION

In our present study, we report that Pin1 is an essential regulator of the self-renewal and maintenance of pluripotent stem cells. We further found the following: 1) Pin1 is induced upon the induction of human iPS cells; 2) the co-expression of Pin1 with defined reprogramming factors significantly enhances the

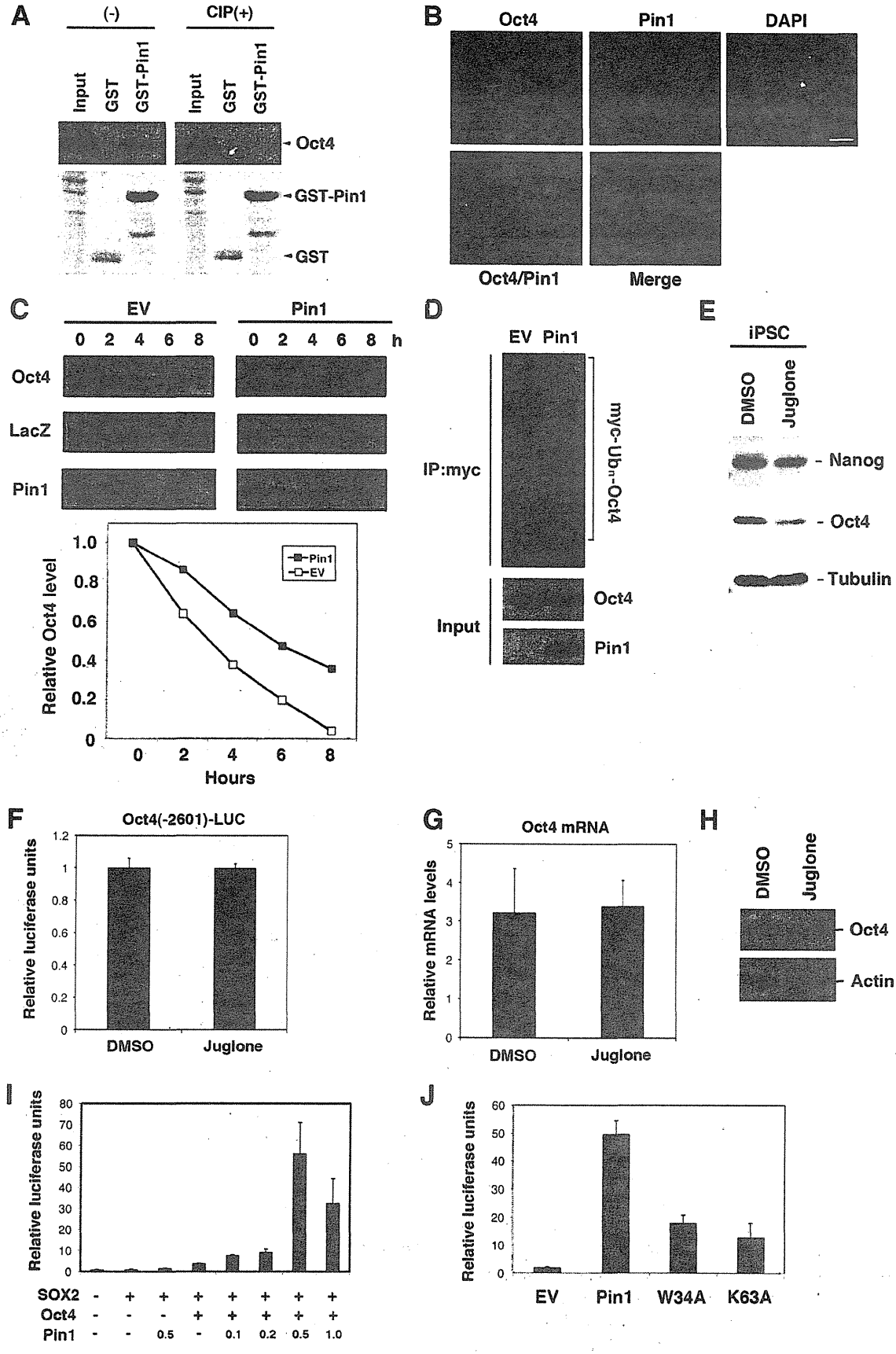

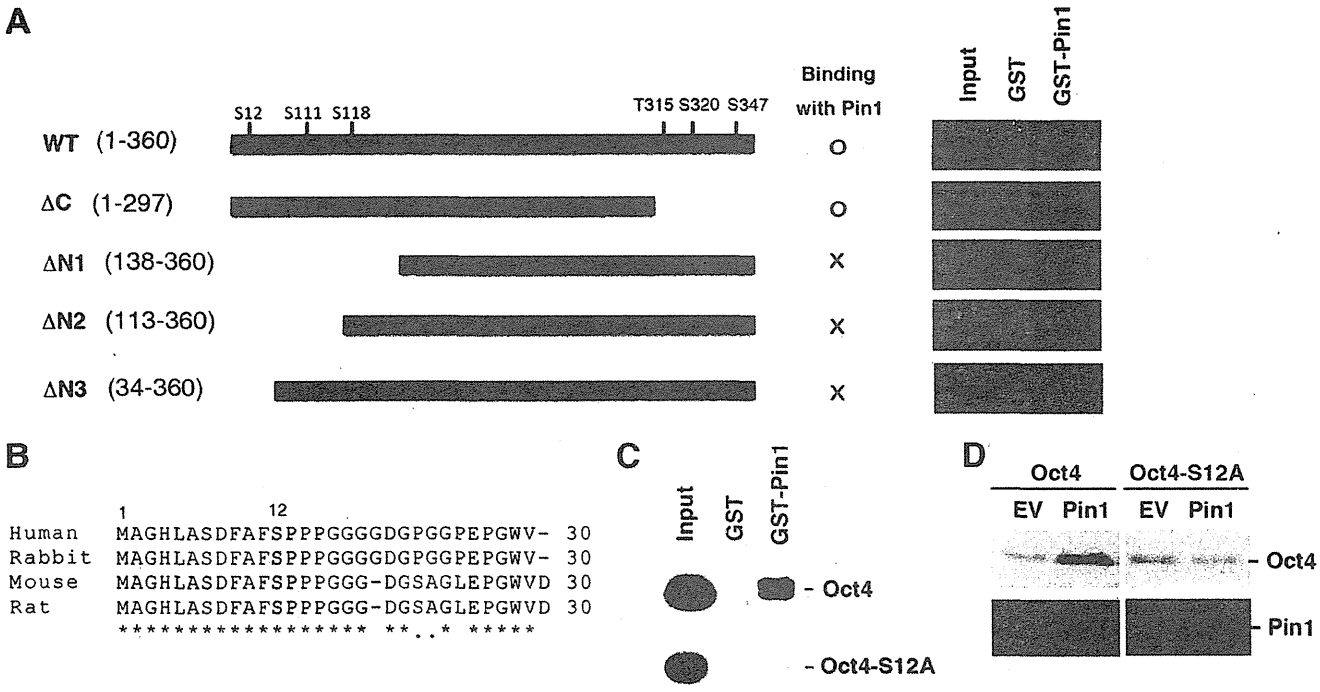

FIGURE 7. **Pin1 interacts with the Ser[12]-Pro motif of Oct4.** *A*, schematic representation of the Oct4 deletion mutants generated in this study (*left panel*). HeLa cells were transfected with the indicated Oct4 deletion mutants for 24 h. Cell lysates were then prepared and subjected to GST pulldown analysis with either GST or GST-Pin1 followed by immunoblotting analysis with Oct4 antibodies (*right panel*). *B*, amino acid sequence alignment of the human, rabbit, mouse, and rat Oct4 proteins. The conserved Ser[12]-Pro motifs are *boxed*. *C*, HeLa cells were transfected with the Oct4 site-directed mutant Oct4-S12A and subjected to GST pulldown analysis. *D*, HeLa cells were transfected with wild-type Oct4 or its S12A mutant with or without Pin1. After 24 h, the cells were subjected to immunoblotting analysis with an anti-Oct4 antibody.

frequency of iPS cell induction; 3) the blockade of Pin1 significantly inhibits the colony formation of dissociated human iPS cells and murine ES cells; 4) Pin1 inhibition leads to the aberrant cell differentiation in human iPS cells and murine ES cells after forming colonies; 5) Oct4 is a putative Pin1 substrate in human iPS cells; and 6) Pin1 interacts with Oct4 at its Ser[12]-Pro motif and facilitates its stability and enhanced transcriptional activity. Our findings thus uncover a novel role of Pin1 as a putative regulator of the self-renewal and survival of pluripotent stem cells via Oct4 function.

Our current results add to previous findings indicating that Pin1 is a multifunctional protein that mediates various phosphorylated proteins involved in divergent cellular processes (17). This implicates Pin1 as a modulator of multiple signaling pathways depending on the cell type and biological context. Indeed, we demonstrate in our present study that Pin1 is a crucial regulator of the phosphorylation-dependent intracellular signaling network that controls cellular stemness and pluripotency. Moreover, iPS cells induced by the expression of four Yamanaka factors (Oct4, SOX2, Klf4, and c-Myc) led to a high expression level of Pin1, and these cells were found to be dependent on Pin1 function. This suggests that Pin1 could be one of the crucial factors in the induction of iPS cells from somatic cells that functions by cooperating with reprogramming transcription factors.

FIGURE 6. **Pin1 interacts with phosphorylated Oct4 and enhances its transcriptional activity.** *A*, human iPS cell lysates treated or untreated with calf intestine alkaline phosphatase were subjected to GST pulldown analysis with either GST or GST-Pin1, followed by immunoblotting analysis with anti-Oct4 antibody (*upper panel*). Coomassie staining for the GST or GST-Pin1 used in the assay is shown in the *lower panel*. *B*, human iPS cells were fixed with 4% paraformaldehyde and then co-immunostained with monoclonal antibodies against Oct4 (*green*) and polyclonal antibodies against Pin1 (*red*). Cells were then analyzed by confocal microscopy. *Scale bar*, 10 μm. *C*, HeLa cells transfected with the indicated vectors and HA-LacZ cells were treated with cycloheximide and harvested at the indicated time points. This was followed by immunoblotting analysis with Oct4, Pin1, and HA antibodies (*upper panel*). Quantitative data are shown in the *lower panel*. *D*, HeLa cells were transfected with Myc-tagged ubiquitin, Oct4, and co-transfected with either empty vector (*EV*) or Pin1. Cells were then treated with MG-132 for 12 h, and lysates were prepared and immunoprecipitated with anti-Myc antibody followed by immunoblotting analysis with anti-Oct4 antibody. Total cell lysates prior to immunoprecipitation (input) were immunoblotted with anti-Pin1 or anti-Oct4 antibody. *E*, human iPS cells were plated on Matrigel-coated feeder-free dishes and treated with either DMSO or juglone (20 μM) for 24 h. Cell lysates were then processed for immunoblotting analysis with anti-Nanog, anti-Oct4, or anti-tubulin antibodies. *F*, a plasmid containing the luciferase (*LUC*) gene flanked with 2601 bp of the Oct4 5′-upstream region was transfected into murine ES cells. The resulting cells were cultured in Matrigel-coated feeder-free dishes and treated with either DMSO or juglone (10 μM) for 24 h, and analyzed by gene reporter assay. *G*, murine ES cells were cultured in Matrigel-coated feeder-free dishes and treated with either DMSO or juglone (10 μM) for 24 h. Total RNAs were then extracted and reverse-transcribed. These preparations were then subjected to quantitative RT-PCR analysis for Oct4. The transcript levels were normalized using GAPDH. *H*, murine ES cells were cultured in Matrigel-coated feeder-free dishes and treated with either DMSO or juglone (10 μM) for 24 h. Cell lysates were then processed for immunoblotting analysis with either anti-Oct4 or anti-β-actin antibody. *I*, HeLa cells were transiently transfected with plasmids encoding Oct4, SOX2, or Pin1 and co-transfected with Oct-SOX reporter gene and pRL-CMV. At 24 h post-transfection, the cells were collected and subjected to a gene reporter assay. *J*, HeLa cells were transiently transfected with an Oct-SOX reporter gene and co-transfected with plasmids encoding wild-type Pin1 or its W34A or K63A mutants, together with Oct4 and SOX2. At 24 h post-transfection, the cells were collected and subjected to a gene reporter assay.